



UNIVERSIDADE D
COIMBRA

Diogo Vasco Gonçalves Rebelo

**IGF1: BETWEEN CARDIAC REGENERATION AND
REPAIR**

VOLUME 1

**Dissertação no âmbito do Mestrado em Biologia Celular e Molecular
orientada pela Doutora Diana Santos Nascimento e apresentada à
Dissertação em Biologia Celular e Molecular
ao Departamento de Ciências da Vida.**

Outubro de 2021

Acknowledgments

Ao longo deste último ano, difícil tanto pessoalmente como para a sociedade em geral, desenvolvi competências e aprendi lições que me certamente irão acompanhar para o resto da vida, contudo eu não as aprendi sozinho e, portanto, escrevo este texto com a esperança de que aqueles que me acompanharam neste percurso possam sentir uma fração da gratidão que sinto por eles.

Em primeiro lugar, quero expressar o meu agradecimento para com a minha líder de grupo Perpétua Pinto-do-Ó, pela oportunidade de integrar o grupo Stem Cells in Regenerative Biology and Repair e assim realizar a componente experimental desta dissertação. A sua gentileza ao lidar comigo e o seu amor pela beleza marcaram-me profundamente.

Em seguida, gostaria de pronunciar o meu mais profundo agradecimento à minha orientadora Diana Nascimento, pois foi sobre a sua alçada que o meu trabalho foi desenvolvido. Estou gravemente endividado para com o conhecimento adquirido resultado da sua mentoria e pelo carinho e o afeto demonstrado ao longo do ano, tanto a mim como à minha plantinha.

Devo também um agradecimento muito forte à pessoa que mais tempo passou comigo, Cassilda Pereira, e à sua eterna paciência. Posso afirmar sem qualquer margem para dúvidas que foi a maior influência em mim ao longo deste ano e que estou imensamente grato tanto pelo conhecimento teórico como técnico adquirido resultado da sua supervisão. E, embora ainda tenha muito para aprender, eu acredito que sou uma pessoa mais competente e completa graças à Cassilda e tentarei emular o exemplo profissional dado, *ipsis verbis*.

Gostaria também de estender os meus sinceros agradecimentos ao grupo inteiro pela sua calorosa receção e excelente cultura de trabalho e amizade. Com especial ênfase à maior Dissertada de todos, a Pipa, que felizmente já podia chamar de amiga antes da minha estadia no Porto e à sportinguista com as sapatilhas mais bonitas a Rita Gomes, que na ausência da Cassilda, sempre me acompanhou e orientou com seu talento e simpatia natural.

Aproveito também para mencionar a Paula Magalhães e as meninas do CCG pela inesperada amizade desenvolvida e por me alegrarem sempre o dia de fazer a PCR.

Agradeço aos meus colegas mais Pinguços de Coimbra, por terem sido uma excelente companhia no breve tempo que tivemos juntos, com especial ênfase ao mais Rijo de todos, Francisco Costa, o meu irmão de curso (adotado como é óbvio) pela sua inestimável companhia e amizade.

Agradeço também a minhas irmãs e afilhadas de Praxe e aos meus colegas de Lisboa. Com especial ênfase ao meu Padrinho Marcelo por me ter acompanhado ao longo de todo o meu percurso académico e ao Cunha, mestre do Showdown, que desde o infantário está lá para mim, sem falhar, ombro a ombro. Obrigado pela vossa amizade!

Aos meus professores, que desde o carinhoso apoio dado antes da apresentação ao público do meu conto de Natal da escola primária às dicas dadas pelos meus professores universitários. E a todos aqueles que me marcaram pelo caminho. A quem um parágrafo nunca fará justiça. Eu aqui vos agradeço pelo trabalho e esforço coletivo.

Por último gostaria de agradecer aos meus pais, que negados de seguirem os seus próprios estudos, entre ambos contabilizam perto de um século de trabalho, de modo que eu pudesse ter acesso aquilo que lhes fora injustamente negado. Espero assim que este documento sirva de espelho à vossa dedicação, pois esta tese é vossa. Eu quero também que saibam quão orgulhoso eu sou de ser vosso filho e quão muito vos amo. Portanto é sem surpresas que vos dedico esta tese.

Funding

This work was funded by European Structural and Investment Fund (ESIF), under Lisbon Portugal Regional Operational Programme and National Funds through Fundação para a Ciência e Tecnologia (FCT) [POCI-01-0145-FEDER-030985].



Resumo Alargado

As doenças cardiovasculares são a principal causa de morte no mundo, contudo pouco progresso tem sido efetuado na restituição da função do tecido danificado em situações de doença ou lesão. Isto é atribuído à limitada capacidade regenerativa do coração, uma vez que os cardiomiócitos, as células fundamentais do coração, não são capazes de se replicarem a uma taxa que compense a perda de tecido.

O enfarte miocárdio corresponde à morte celular generalizada resultante de uma lesão isquêmica. Caracterizada pelo bloqueio súbito das artérias coronárias (vasos sanguíneos responsáveis por levar o sangue ao coração) levando à falta de oxigênio e nutrientes que chegam ao tecido cardíaco. Para evitar a rutura do tecido, causada pelo espaço vazio deixado pela morte celular pós-lesão, forma-se uma cicatriz fibrosa secretada pelos fibroblastos cardíacos residentes. A fibrose cardíaca é constituída por deposição aberrante de matriz extracelular, rica em colagénio, que apesar de ter uma função estrutural essencial, também contribui para a insuficiência cardíaca e está associada a prognósticos negativos.

Contrariamente aos animais adultos, os murganhos neonatais apresentam uma breve janela de tempo para a regeneração cardíaca. Assim, no primeiro dia do nascimento (P1) o coração é capaz de regenerar ativando a proliferação de cardiomiócitos. Ao contrário, no dia 7 pós-natal (P7), esta capacidade já não é observada. Resultando numa resposta reparatória com formação de fibrose cardíaca. Presentemente, o papel dos fibroblastos cardíacos e da matriz extracelular por si produzida na regeneração e na transição para uma fase reparatória é desconhecido. O que é particularmente importante considerando que os fibroblastos desempenham um papel significativo na remodelação cardíaca.

Os resultados do nosso grupo mostraram que a expressão do transcrito que codifica o fator de crescimento semelhante à insulina 1 ou IGF1 está aumentada entre P1 e P7. IGF1 é conhecido por ser capaz de induzir a proliferação e sobrevivência celular em cardiomiócitos e fibroblastos cardíacos.

Subsequentemente, utilizamos um modelo de cultura celular de fibroblastos cardíacos humanos (FCH), e dois modelos de enfarte do miocárdio (EM) de murganho, um modelo adulto (de reparação) e um modelo neonatal (de regeneração) para descobrir o papel do IGF1 no processo reparador e de regeneração, respetivamente.

No modelo adulto, observamos um aumento da expressão de IGF1 na região do coração sujeita EM 96 horas pós lesão quando comparado com o controlo. Contrariamente, no modelo de lesão neonatal, a expressão de IGF1 diminuiu em comparação com o controlo.

Usando o protocolo de ativação de FCH avaliamos o papel do IGF1 na ativação de FCH. Apesar de ao nível transicional o aumento da expressão de genes associados á ativação de fibroblastos em resposta do tratamento com IGF1 ser modesto, ao nível da proteína verificou-se um aumento significativo de α -SMA (marcador de ativação de fibroblastos cardíacos), indicando que o IGF1 induz a ativação de fibroblastos cardíacos. Paralelamente, por meio de um ensaio de hipoxia, demonstramos que o IGF1 é capaz de proteger o HCF da apoptose induzida por hipoxia, que é um dos componentes da lesão isquémica.

Em suma, descobrimos que o IGF1 tem um papel importante na resposta à lesão isquémica cardíaca e induz ativação de FC, podendo o seu aumento no período neonatal estar envolvido na transição regeneração-reparação.

Palavras-Chave: Doenças Cardiovasculares; Coração; IGF1; Reparação; Regeneração.

Abstract

Cardiovascular diseases are the leading cause of death worldwide, with ischemic heart disease being the most prevalent, yet no breakthrough in restoring healthy tissue function has been achieved. In part, this has been attributed to the limited regenerative capacity of the heart since cardiomyocytes after an injury do not replicate at a sufficient rate for regeneration to occur.

Myocardial Infarction, or MI, is the widespread cell death resulting from an acute ischemic injury following sudden blockage of the coronary arteries, leading to a lack of oxygen and nutrients reaching the myocardium. To prevent the tissue rupture caused by the hollow space left out by the cell death post-injury, a collagen-rich fibrous scar is formed by the abnormal deposition of the extracellular matrix (ECM) by cardiac fibroblasts (CF). Although essential, this provides structural support to the myocardial wall after injury, cardiac fibrosis also contributes to heart failure and is associated with poor clinical outcomes.

However, work in mice showed a brief time window for heart regeneration: at postnatal day 1 (P1), the heart regenerates by the proliferation of cardiomyocytes, while at postnatal day 7 (P7), it engages on a repair response. Yet, the role of CF and their produced ECM in this transition is still unknown. This is especially important considering CFs are known to play a significant role in cardiac remodeling.

Herein, using RNA-sequencing, we showed that insulin-like growth factor 1 or IGF1, an ECM-associated protein secreted by CF, is up-regulated between P1 and P7. IGF1 is known to induce cell proliferation and survival in CMs and CFs. Following this, we combined an *in vitro* human CF (HCF) activation protocol with adult (Repair model) and neonatal (Regenerative model) MI mouse models to unveil the role of IGF1 in repair and regeneration, respectively.

We observed an upregulation of IGF1 expression in different heart regions after MI in the adult MI model. Contrarily, IGF1 expression was downregulated following neonatal MI. These findings demonstrate that IGF-1 may be essential for the repair process and that IGF1 knockdown may be determinant for effective regeneration.

Using an activation protocol of HCF, we measured the impact of IGF1 on CF activation and found that although not very evident at the transcriptional level, IGF1 was able to increase the number of α -SMA-expressing cells supporting IGF1 capability to induce fibroblast activation. Furthermore, we demonstrated that IGF1 is capable of protecting HCF from hypoxia-induced apoptosis.

Briefly, we found that IGF1 has an important role in response to cardiac ischemic injury, is capable of CF activation and that its modulation may be of therapeutic significance.

Keywords: Cardiovascular Diseases; Heart; IGF1; Repair; Regeneration.

Index

| | |
|--|------|
| Acknowledgments..... | II |
| Funding | IV |
| Resumo Alargado..... | V |
| Abstract | VII |
| List of Tables | XIII |
| List of Abbreviations | XIV |
| Introduction..... | 17 |
| Heart..... | 17 |
| ECM..... | 18 |
| Cardiac Fibroblasts | 18 |
| The Adult Heart Repair after MI | 19 |
| <i>Inflammatory Phase</i> | 20 |
| <i>Reparative or Proliferative Phase</i> | 21 |
| <i>Maturation Phase</i> | 21 |
| On the regeneration of the myocardium | 22 |
| The insulin-like growth factor family | 24 |
| IGF1 effects in cardiomyocytes | 26 |
| IGF1 effects on Cardiac Fibroblasts | 27 |
| Objectives..... | 28 |
| Materials and Methods..... | 29 |
| Animal model and ethical statement..... | 29 |

| | |
|---|----|
| Targeted Transcriptome Sequencing | 29 |
| Myocardial Infarction by permanent ligation model in adult mice | 29 |
| Myocardial Infarction by permanent ligation model in neonatal mice | 30 |
| Histology Masson trichrome | 31 |
| Cell Culture | 31 |
| Cardiac fibroblasts activation assays | 32 |
| RNA isolation | 32 |
| Real-Time qPCR..... | 33 |
| Immunofluorescence..... | 34 |
| Survival Assay | 35 |
| Western Blot | 36 |
| Data and statistical analysis | 37 |
| Results | 38 |
| <i>Igf1</i> and <i>Igf2</i> are differently expressed during the cardiac regeneration-repair transition | 38 |
| <i>Igf1</i> expression is increased in mice after MI..... | 40 |
| <i>Igf1</i> and <i>Igf2</i> expression is decreased during neonatal heart regeneration..... | 43 |
| IGF1 expression is increased during in vitro cardiac fibroblast activation | 44 |
| IGF1 role on human cardiac fibroblast activation..... | 46 |
| IGF1 has a protective effect against hypoxia-induced apoptosis in human CFs | 49 |
| Discussion | 51 |
| Conclusion and future perspectives | 57 |
| References | 58 |

| | |
|--|----|
| Supplementary Data | 71 |
| Supplementary materials | 71 |
| Quantification of IGF1 in human pericardial fluid and plasma by ELISA..... | 71 |
| Supplementary figures | 72 |

List of Figures

| | |
|--|----|
| Figure 1 – Three main phases of the cardiac injury..... | 22 |
| Figure 2 – <i>Igf1</i> and <i>Igf2</i> transcription is altered in the heart during the transition from regeneration to repair - | 40 |
| Figure 3 – IGF family is differently expressed after MI in adult mice..... | 42 |
| Figure 4 – <i>Igf1</i> and <i>Igf2</i> expression decreases with time after MI in neonatal (P1) mice | 44 |
| Figure 5 – IGF1 expression is increased in activated cardiac fibroblasts | 46 |
| Figure 6 – IGF1 is able to induce HCF activation | 48 |
| Figure 7 – IGF1 has a protective effect against hypoxia-induced apoptosis in human CFs | 50 |

List of Tables

| | |
|---|----|
| Table 1 - Primer sequences for qRT-PCR..... | 33 |
| Table 2 - qRT-PCR cycling conditions | 34 |

List of Abbreviations

| | Abbreviations |
|---|----------------------|
| 4,6-diamidino-2-phenylindole | DAPI |
| Ascorbate-2-phosphate | Asc 2-P |
| Bovine serum albumin | BSA |
| Bromodeoxyuridine | BrdU |
| Cardiac fibroblasts | CF |
| Cluster of differentiation 90 | CD90 |
| Danger-associated molecular patterns | DAMPs |
| Day | D |
| Days post-injury | dpi |
| Deoxyribonucleic Acid | DNA |
| Differentially expressed genes | DEG |
| Direção Geral de Alimentação e Veterinária | DGAV |
| Dulbecco's Modified Eagle Medium | DMEM |
| Embryonic | E |
| Enzyme-linked immunosorbent assay | ELISA |
| Extracellular matrix | ECM |
| False Discovery Rate | FDR |
| Fetal Bovine Serum | FBS |
| Fibroblast Growth Medium | FGM |
| Field of view | FOV |
| Growth hormone | GH |
| Heart failure | HF |
| High mobility group box-1 | HMGB1 |
| High-temperature requirement A serine peptidase | HTRA |
| Horseradish Peroxidase | HRP |
| Human Cardiac Fibroblasts | HCF |
| Infarct zone | IZ |
| Insulin-like growth factor 1 | IGF1 |
| Insulin-like growth factor 2 | IGF2 |
| Insulin-like growth factor 1 Binding Protein | IGFBP |
| Insulin-like growth factor 1 Receptor | IGF1R |
| Interleukin | IL |

| | |
|---|-----------------|
| Intraperitoneally | IP |
| Left anterior descending | LAD |
| Left ventricular | LV |
| Mouse cardiac fibroblasts | mCF |
| Myocardial infarction | MI |
| NOD-like receptors | NLRs |
| Paraformaldehyde | PFA |
| Pattern recognition receptors | PRRs |
| Phosphate-buffered saline | PBS |
| Platelet-derived growth factor receptor- α | PDGFR- α |
| Penicillin/Streptavidin | P/S |
| Postnatal | P |
| Post-translational modifications | PTM |
| Principal component analysis | PCA |
| Radioimmunoprecipitation assay | RIPA |
| Reactive oxygen species | ROS |
| Real-time Polymerase Chain Reaction | qRT-PCR |
| Remote zone | RZ |
| Ribonucleic acid | RNA |
| Room temperature | RT |
| Stem cells antigen-1 | Sca1 |
| Transcription factor 21 | TCF21 |
| Transforming growth factor beta 1 | TGF- β 1 |
| Toll-like receptors | TLRs |
| Tris-buffered saline | TBS |
| Tdt-mediated dUTP nick-end labelling | TUNEL |
| Vascular endothelial growth factor | VEGF |
| Yes-associated protein | YAP |

“The animal’s heart is the basis of its life, its chief member, the sun of its microcosm; on the heart, all its activity depends, from the heart all its liveliness and strength arise.”

William Harvey, *De Motu Cordis* (1628)

Introduction

Nearly 400 years since William Harvey set the cornerstone of modern-day cardiology, heart disease is still the leading cause of death worldwide¹. Coronary heart disease and its sequelae, including myocardial infarction (MI) and heart failure (HF), represent the bulk causes of this lethality¹.

Coronary heart disease (or ischemic heart disease) is a pathology characterized by the narrowing or blockage of the coronary arteries lumen. The coronary arteries are the blood vessels that carry blood to the heart. Atherosclerosis is usually the leading cause of coronary heart disease. Atherosclerosis (the hardening or the clogging of arteries) refers to fibrous lesions and the accumulation of fatty deposits (called plaques) in the artery wall. As the atherosclerotic plaque increases in size, it can reduce, obstruct, or stop blood flow to the heart muscle. If the heart does not get enough blood, it cannot get the oxygen and nutrients it needs to work correctly. MI, or as it is commonly referred to as heart attack, happens when a coronary artery becomes abruptly blocked, stopping the blood flow to the heart, damaging it in the process².

MI is characterized by acute necrosis of cardiomyocytes in the ischemic myocardium, with the following generation of a reparative fibrotic scar that, although necessary to prevent ventricular wall rupture, in the long-run aids in the establishment of HF, as interstitial fibrosis accumulates throughout the heart, leading to wall and septal stiffening and progressively worsening cardiac function³. Therefore, understanding the mechanisms behind fibrosis is necessary so that we may safeguard ourselves from excessive scarring.

Heart

The mammalian heart is a muscular organ that pumps blood through the circulatory system. It has four chambers, with the upper most two named atria, while the lower chambers are named the ventricles⁴. It is further composed of three distinct layers: pericardium, myocardium, and endocardium. The epicardium is a single continuous layer of the mesothelium that outlines the heart and comes into contact with the pericardial cavity, which contains a fluid named pericardial fluid, which lubricates the heart⁵. Whereas the endocardium lines the interior of the heart⁴, the myocardium is mainly comprised of cardiomyocytes (contractile muscle cells) and supporting stroma cells such as cardiac fibroblasts (CF), endothelial cells, mural cells, and immune cells⁴.

ECM

One other important component of the heart is the extracellular matrix (ECM) which is a complex and dynamic network of molecules, ranging from proteins, such as collagens, to glycoproteins, such as fibronectin and proteoglycans⁶. These molecules are secreted locally by cells and remain strongly associated with them, providing structural (e.g., collagen and elastin), adhesive (e.g., fibronectin), and biochemical signaling support⁷. The ECM partly regulates cell behavior by influencing proliferation, survival, shape, migration, and differentiation⁸, with both cardiomyocytes and noncardiomyocytes being enmeshed in a network of ECM proteins⁹. One of the main functions of the ECM is to provide tissue integrity and structural support, being 90% of the structural meshwork is composed of collagen type I or type III¹⁰.

The ECM also serves as a milieu to matricellular proteins¹¹. Unlike structural matrix components (e.g., collagen and elastin), matricellular proteins do not provide mechanical support but bind to matrix proteins and cell receptors, transducing signaling cascades^{12,13}. Because matricellular proteins can modulate all involved cells' behavior and function in a myriad of processes, in roles as varied as intervertebral disc function (through cell-ECM interactions and ECM synthesis)¹⁴, priming the tumor microenvironment (initiating signaling events associated with cancer development)¹⁵, and maintaining homeostasis in inflammation and immunity (modifying immune substrates or cleaving transmembrane receptor)¹⁶ they have become desirable therapeutic targets^{17,18}. In the cases of the heart, the interstitial matrix is also a transducer of molecular signals, playing an active role in regulating development¹⁹, sustaining normal organ function, and inflammatory and reparative responses²⁰.

Cardiac Fibroblasts

CFs are cells of mesenchymal origin capable of the production of connective tissue²¹. This dynamic cell type is responsible for most ECM deposition and maintenance²². They are further characterized for their extensive rough endoplasmic reticulum and sizeable Golgi apparatus, and oval nucleus²². Their primary function is tissue support producing a mechanical scaffold for cardiomyocytes²¹. CF can also change the neighboring cell's electrophysiology by enabling cell to cell communication with cardiomyocytes and endothelial cells through GAP junctions, or physically isolating the cells, thus creating conduction barriers^{23,24}. Although past studies suggested that activated fibroblasts in the heart originated from a wide array of unrelated cell types like endothelial cells, bone-marrow progenitor cells, or pericytes that underwent a process of transdifferentiation²⁵. This former paradigm has disregarded the presence of fibroblasts already residing in the myocardium and their capacity to mediate tissue remodeling and ECM production. According to Tallquist and Molkenin the transdifferentiation hypothesis would lack rapid responsiveness and homogenous spatial coverage

throughout the tissue²⁶, and contrariwise the resident fibroblasts are geometrically interspersed between cardiomyocytes and hold the appropriate molecular program to allow prompt responsiveness after injury²⁶.

The previous paragraph's theoretical framework, coupled with the recent development of genetic mouse models (with CF-specific allele expression of Cre recombinase)²⁷⁻²⁹ and multicolor flow-cytometry^{30,31}, has helped define the role and heterogeneity of CF. Hence, several CF markers have emerged, namely CD90 (cluster of differentiation 90), Sca-1 (stem cells antigen-1), PDGFR- α (platelet-derived growth factor receptor- α), and TCF21 (transcription factor 21). For example, lineage tracing of TCF21 expressing cells has shown that CFs that express this transcription factor³¹ originate from the epicardium during development²⁹ and give rise to most injury-activated fibroblasts²⁷. The current consensus is that 80% of injury-activated, matrix-producing cells seem to expand from tissue-resident fibroblasts poised to respond³².

Cardiac fibroblast activation occurs in response to cardiac injury and inflammation. As defined in cultured fibroblasts, a central cytokine involved in fibroblast activation is TGF- β 1³³. In the canonical pathway, TGF- β 1 binds to and causes heterodimerization of TGF- β 1 receptors 1 and 2, which induces direct phosphorylation of SMAD2 and SMAD3. Both then translocate to the nucleus in complex with SMAD4 to promote fibroblast differentiation-specific gene expression^{26,33}. The non-canonical pathways involve the Ras/ERK; JNK/p38; Rho-like GTPases, and PI3K/AKT pathways^{34,35}. TGF- β 1 also promotes a profibrotic environment by upregulating microRNAs associated with a fibrotic response such as microRNA (miRNA)-21^{36,37} or by downregulating anti-fibrotic miRNAs such as let-7^{37,38}. Activation of fibroblasts induces transcriptional activity of the *ACTA* gene leading to the appearance of smooth muscle α -actin (α -SMA) stress fibers that confer cells mechanical integrity and contractile capacity³⁹. Fully activated fibroblasts are named myofibroblasts. The latter are phenotypically modulated fibroblasts that are larger than a nonactivated fibroblast, develop stress fibers, present high contractility ability (through the expression of contractile proteins), and secrete different types of structural proteins (mainly collagen type I and III) and numerous cytokines, all necessary for effective wound healing^{26,40,41}.

The Adult Heart Repair after MI

Although cardiomyocyte renewal is observed throughout the lifespan, this renewal is modest⁴². This is why the heart, unlike other organs, has limited regenerative capacity⁴². In the case of myocardial ischemia resultant from a MI, massive loss of cardiomyocytes overwhelms the myocardium's limited regenerative capacity, causing a fibrotic scar formation³.

The cardiac repair response to MI can be roughly divided into three phases (Figure 1). The inflammatory phase is characterized by an intense inflammatory response triggered by danger signals released by dying cells⁴³. The second phase is called the reparative or proliferative phase and is characterized by immunomodulation, myofibroblast proliferation, collagen deposition, scar formation, and neovascularization, thereby resulting in wound healing⁴⁴. The maturation phase follows the collagenous matrix becoming crosslinked and a significant part of the myofibroblast population becoming apoptotic⁴⁴.

Inflammatory Phase

As hypoxia sets in, necrotic, stressed, or injured cells release substances that act as danger signals, termed danger-associated molecular patterns (DAMPs)^{45,46}. DAMPs bind to pattern recognition receptors (PRRs) of the innate immune system of infiltrating leukocytes and surviving cells and activate a cascade of inflammatory mediators, including inflammatory cytokines, chemokines, and cell adhesion molecules⁴⁶. On top of being passively released by cell death or damage to the ECM, DAMPs may also be actively secreted by stressed cardiomyocytes, fibroblasts, or activated leukocytes. Some examples of these DAMPS are high mobility group box-1 (HMGB1)⁴⁷, fibronectin extra domain A, interleukin (IL)-1 α , hyaluronic acid, and multiple nucleic acids^{48,49},

PRRs consist mainly of membrane-bound Toll-like receptors (TLRs), IL-1Rs, and nucleotide-binding oligomerization domain (NOD-like receptors or NLRs)⁵⁰. The signaling pathways downstream of these PRRs have been comprehensively detailed in recent reviews^{51,52}.

Downstream signaling converges on the activation of ERK and NF- κ B. These pathways drive the expression of a large panel of pro-inflammatory genes, including inflammatory cytokines and chemokines (that attract monocytes and T-lymphocytes)⁵⁰ and cell adhesion molecules (e.g., vascular cell adhesion molecule, intercellular adhesion molecule)^{51,52}.

The resulting leukocyte recruitment further magnifies the inflammatory response (these effects are partly mediated by M1 phenotype macrophages⁴⁴), increasing the production of DAMPs and promoting both efferocytosis of dying cells and tissue digestion via the release of proteases and oxidases. Efficient efferocytosis of apoptotic cardiomyocytes is crucial for transitioning from the inflammatory to the resolution and wound healing phases⁵³.

Despite the relevance of the inflammatory phase for the clearance of dead cells and debris, its timely suppression and spatial containment are necessary for effective wound healing. This event is dependent on the release of secreted anti-inflammatory mediators and activation of intracellular

signals that inhibit the innate immune response⁵⁰. Defects in the molecular pathways responsible for suppressing and resolving the inflammatory response may be involved in the pathogenesis of adverse remodeling of the heart⁵⁴.

Reparative or Proliferative Phase

During this phase, which begins around day 3 post injury⁴⁴, transient and highly plastic ECM rich in fibrin and fibronectin is formed and serves as a scaffold for migrating and proliferating cells⁵⁵. Resident CFs are recruited to the injury site, become activated, and undergo myofibroblast transdifferentiation^{44,56} (see above, “Cardiac Fibroblast” section). These proliferate through the provisional ECM to the wound site and secrete large amounts of collagens (mostly collagen types I and III) which maintain the structural integrity of the infarcted ventricle^{57,58} and the provisional matrix is degraded⁵⁹. Besides the deposition of structural ECM proteins, CFs are also responsible for the synthesis and secretion of matricellular proteins (absent from healthy tissue). Although these have no scaffolding function, they serve to modulate cell function and promote proper matrix assembly^{44,59}.

At the same time, new capillary vessels (angiogenesis) mediated by the vascular endothelial growth factor (VEGF) are being formed to deliver oxygen and nutrients to the infarcted area, as this is essential for the recovery of the tissue after ischemic injury⁶⁰. This action is being potentiated by infiltrated M2 macrophages that express anti-inflammatory, pro-fibrotic, and angiogenic factors⁴⁴.

Maturation Phase

The proliferative phase of cardiac repair is followed by scar maturation, as the collagen in the extracellular matrix becomes crosslinked⁶¹, and reparative myofibroblasts are deactivated and may undergo apoptosis⁶².

The molecular signals involved in the quiescence of these myofibroblasts remain unexplained. The withdrawal of fibrogenic growth factors, the activation of inhibitory stop signals that terminate TGF- β 1 and angiotensin II signaling,^{63,64} and the clearance of matricellular proteins¹² may be the cause since a reduction in myofibroblast density during the maturation phase has been thoroughly documented^{65,66}.

Therefore, we can affirm that when fibroblasts become activated into myofibroblasts in response to MI, ECM is produced to maintain the heart's structure. However, when excessive ECM is deposited, cardiac insufficiency can ensue due to the formation of a fibrotic scar²⁶.

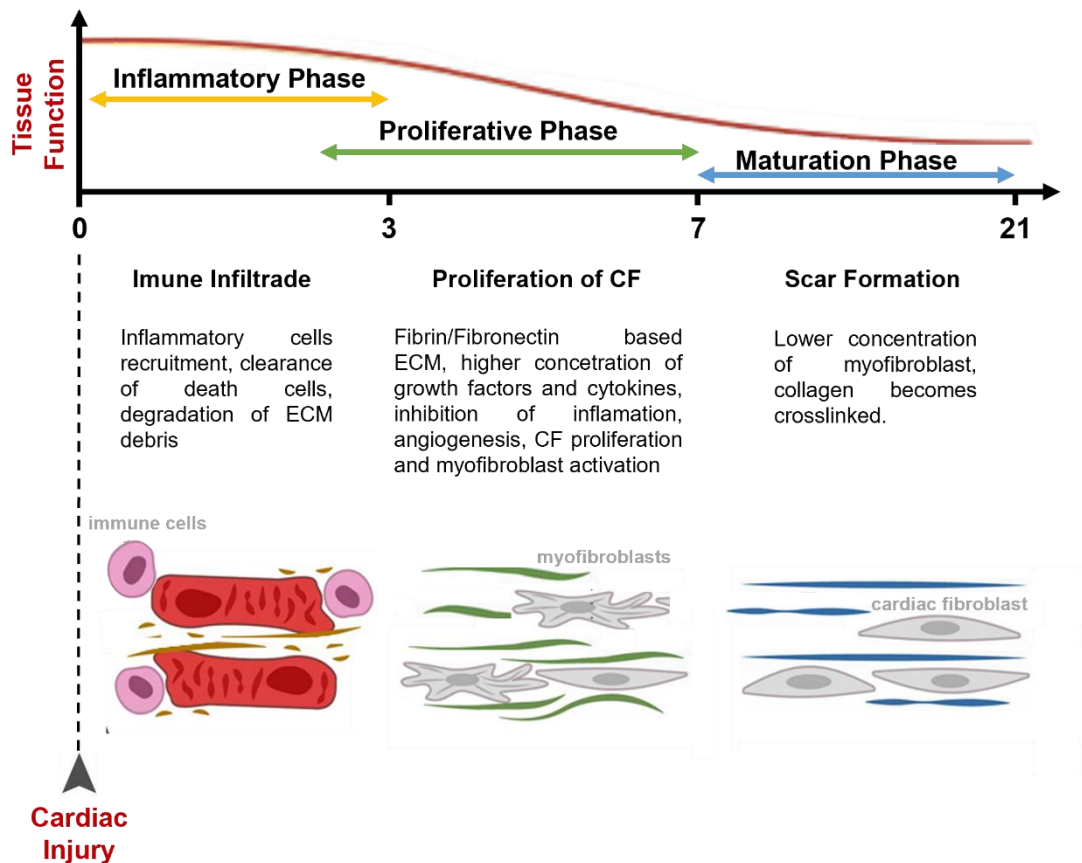


Figure 1 – Three main phases of the cardiac injury –Adapted from Silva et al. 2020⁵⁹.

On the regeneration of the myocardium

Regeneration occurs when lost or damaged tissues, organs, or limbs are re-formed from the remaining tissue, keeping their original function and tissue integrity⁶⁷.

There are multiple possible means by which injured tissues regenerate⁶⁸. First, new cell types could be produced by resident stem cells⁶⁹. Second, new cells could be originated through dedifferentiation - loss of a cell type's differentiated character - to form a dividing cell that acts as a progenitor cell⁷⁰. Lastly, differentiated cells could divide to produce more cells⁷¹.

Unlike adults, mouse neonates on the first day of life (P1) can regenerate their hearts after injury, forming new functional tissue by activating cardiomyocyte' proliferation⁷². This response is no longer observed one week after birth (P7) when a repair process is observed⁷². This transition from a regenerative to a reparative injury response seems to coincide with the maturation of cardiomyocytes characterized by a phenotypic switch from hyperplastic (cell division) to hypertrophic (cell size) cellular growth, binucleation, and subsequently cell cycle withdrawal⁷³.

However, the root triggers of binucleation are still rather ill-defined⁷⁴. The transition from energetic pathways from embryonic glycolytic metabolism to postpartum oxidative phosphorylation leading to reactive oxygen species (ROS) accumulation is a widely accepted hypothesis^{75,76}. However, other causes have been suggested, such as thyroid hormone sensing⁷⁷ and cardiac pressure overload^{78,79}.

The current regeneration paradigm came about as both urodele amphibians, and teleost fish showed a remarkable capacity for cardiac regeneration throughout life⁸⁰⁻⁸². Adult zebrafish, for example, can undergo complete cardiac regeneration without scar formation after resection of up to 20% of the ventricle, a response thought to occur primarily through cardiomyocytes proliferation⁸³. Given the similarities between the embryonic/immature mammal heart and the adult zebrafish heart, Porrello and colleagues hypothesized that the cell regulation mechanism responsible for regeneration could be conserved in the early mammalian heart⁷².

This insight proved to be fortuitous since, after apex resection on P1, Porrello's group observed cardiomyocyte mitosis and cytokinesis coupled with sarcomere disassembly. These findings were consistent with the idea that the regenerative potential of heart tissue in neonatal mice involved widespread dedifferentiation and proliferation of existing cardiomyocytes⁶⁸. Alas, myocardium regeneration was no longer present at P7 as a repair response readily developed⁷².

To better understand said mechanisms, several models of neonatal cardiac injury had been established, namely apex resection⁸⁴, cryoinjury⁸⁵, and MI (by coronary artery ligation)⁸⁶; and all have proven to activate regenerative mechanisms at various extents. However, MI is the injury model with higher translational potential, and after this injury, complete regeneration has been consistently reported^{86,87}.

However, our understanding of the ECM's role in the regenerative and reparative response remains limited. Recently Ángel Raya's group showed that ECM stiffness is crucial in determining the neonatal mouse heart's regenerative potential and perhaps more critical than the cell-associated mechanisms behind the switch from a regenerative to a repair response, which occurs sooner than day 7, at around postnatal day 2⁸⁸. Moreover, through decellularization experiments, it was shown that the heart ECM from regenerative periods has a different composition than that of reparative periods⁸⁹, namely being richer in fibronectin, which has previously been referenced as a promoter of regeneration by promoting cardiomyocyte proliferation⁹⁰. Additionally it was reported that the ECM protein agrin is able to promote cardiac regeneration by activating the Yes-associated protein (YAP) signaling pathway⁹¹ and subsequent cardiomyocyte re-entry in the cell cycle⁹¹.

Plus Wang et al.⁹² reported that adult CFs secreted proteins can induce significant cardiomyocyte maturation. This understanding was achieved through a single-cell RNAseq of mice at multiple post-natal periods and by a co-culture of neonatal mouse cardiomyocytes and human embryonic stem cell-derived cardiomyocytes with the corresponding adult cardiac fibroblasts.

These works linking ECM and CFs secreted proteins to cardiac regeneration give strength to the possibility of channeling these cell regulation mechanisms and inducing them later and restoring cardiac function to patients with heart failure⁹³.

The insulin-like growth factor family

Insulin-like growth factor-1 or IGF1 is a growth factor that triggers an intracellular signal-transduction pathway leading to differentiation, proliferation, or other cellular response⁹⁴. IGF1 is a 7kDa, 70 amino acid polypeptide chain, cross-linked by three disulfide bonds. Both its sequence and resulting tertiary structure are structurally and functionally related to the insulin hormone, sharing 48% homology⁹⁵. IGF1 acts as a ligand for insulin-like growth factor-1 receptor or IGF1R⁹⁶, leading to the activation of the intrinsic tyrosine kinase activity, which auto-phosphorylates tyrosine residues thus initiating a cascade of down-stream signaling events involved in cell growth, apoptosis, autophagy, and aging⁹⁷.

IGF1 is part of the IGF family of proteins. This family comprises two ligands, IGF1 and IGF2, seven associated binding proteins, IGFBP 1-7, three IGFBP associated proteases, named high-temperature requirement A serine peptidases HTRA1-3 and two distinct receptors IGF1 receptor and IGF2 receptor (IGF1R and IGF2R respectively)⁹⁸.

The IGF1 coding gene has 6 exons, and it is alternatively spliced into two classes of transcripts. However, after processing, all isoforms give rise to the same mature protein^{99,100}. Therefore, it is suggested that the different classes of transcripts can be associated with IGF1 regulation. Namely, that class 2 transcript possesses a motif associated with efficient secretion in the liver, while the class 1 transcript does not and is associated with an autocrine/paracrine action^{99,101}.

The IGF1 found in circulation is mainly synthesized and secreted by the liver in response to hypothalamic growth hormone (GH) signaling¹⁰². However, other tissues can produce IGF1, which acts locally as an autocrine and paracrine hormone. These actions are thought to underpin the regulation of cells growth, proliferation, and survival¹⁰³. The main synthesizers of IGF1 in the heart are believed to be the cardiac fibroblasts¹⁰⁴.

IGF1 is substantially regulated by IGF binding proteins (IGFBPs) and by IGFBP associated degrading enzymes^{105,106}, from the seven known forms IGFBP described IGFBP1-6 being high affinity and

IGFBP7 being a low-affinity binding protein)¹⁰⁷. These proteins bind to IGF1 with an equal or greater affinity than the IGF1 receptor (IGF1R) and thus can modulate the outcomes of its signaling¹⁰⁶. However, their actions are not equal as the most prevalent binding protein in the bloodstream IGFBP3 stabilizes IGF1 in circulation¹⁰⁸, while IGFBP4 has been known to interfere with IGF1 and IGF1R interaction, hence having a negative impact on its signaling¹⁰⁷. The effects of the binding proteins are contrasted by the action of IGFBP associated degrading enzymes, which degrade and hence counteract the effects of the IGFBPs, especially HTRA1¹⁰⁵. The balance caused by these two classes of proteins is partially responsible for IGF1 bioavailability and its interaction with IGF1R¹⁰⁶.

Insulin-like Growth Factor-2 is structurally similar to IGF1. IGF2 expression is mainly circumscribed to the embryonic period^{109,110}. While IGF1 is expressed throughout life, peaking in adolescence/early adulthood and slowly declining with age^{111–113}. Most of the proliferative effects for both IGF1 and IGF2 can be attributed to the IGF1R pathway since IGF2 can also bind to IGF1R¹¹⁴. Interestingly, IGF2 has been reported to support cardiac regeneration in neonatal mice¹¹⁵. These insights were accomplished through IGF2 knock-out mice not regenerating but the paracrine introduction, IGF2 rescuing the regenerative phenotype¹¹⁵.

The structure of IGF1R is comprised of an $\alpha 2\beta 2$ heterotetrameric complex of approximately 400 kDa. IGF1R has two extracellular subunits that contain ligand-binding sites. Each subunit couples to one of the two membrane-spanning subunits containing an intracellular domain with intrinsic tyrosine kinase activity¹¹⁶. The binding of IGF1 to its receptor initiates a complex signaling cascade⁹⁶. IGF1R is significantly regulated¹¹⁷, mostly through receptor internalization however, post-translational modifications such as ubiquitination have also been reported contributing to a higher dynamism of the pathway¹¹⁸.

The two major pathways involved in the IGF1R signaling in the heart are the PI3K-AKT and the Ras-ERK pathway. Activating PI3K-AKT signaling cascade leads to a downregulation of FOXO genes (resulting in an inhibition of autophagy) and an upregulation of both mTOR1 and mTOR2 genes¹¹⁹. These effects are thought to underlie both the cell growth (hypertrophy) and the aging mechanisms associated with IGF1R signaling¹²⁰. The activation of the Ras-ERK pathway has been linked to cell growth, proliferation, and antiapoptotic effects¹²¹. Both pathways have been reported to be non-canonical pathways of the TGF- β 1 signaling^{34,35} and have been extensively studied and thoroughly reviewed and we will not delve into them further^{119,121,122}.

IGF1 effects in cardiomyocytes

Epidemiological studies on the cardiovascular system report that a lack of circulating IGF1 has an adverse clinical outcome¹²³, specifically associated with a higher prevalence of ischemic heart disease¹²³. This suggests that IGF1 can have a protective role in the cardiac setting, and several studies reinforce this observation. Duerr et al. demonstrated that treatment with IGF1 in rats with left ventricular (LV) dysfunction after MI showed a marked up-turn on cardiomyocyte hypertrophy¹²⁴. This hypertrophic response leads to a restoration of function of the cardiac tissue and is widely accepted as a compensatory mechanism for the loss of cardiomyocytes after injury¹²⁵. Q Li et al. found that overexpression of IGF1 in mice protected cardiomyocyte cell death after ischemic injury¹²⁶, consistent with the signaling mechanisms of IGF1R¹²¹. Also, in a transgenic mouse model expressing IGF1 restrictively on the heart, after MI, cardiac repair and regeneration occurred more efficiently than in the wild-type mice with higher cardiomyocyte proliferation and a smaller scar being formed¹²⁷.

Other studies have also found that IGF1 has a positive role in cardiac remodeling¹²⁸. Interestingly, these effects were not mediated through the IGF1R of cardiomyocytes but the modulation of the surrounding microenvironment through the targeting of IGF1R of macrophages infiltrated in the tissue post-injury, leading to the establishment of a pro-repair M2 phenotype¹²⁸. A similar targeting of IGF1R in macrophages was found in the regeneration of skeletal muscle¹²⁹.

Meanwhile, Baez-Diaz et al. and O'Sullivan et al. found that porcine hearts treated with IGF1 after MI display a significant improvement of cardiac function and limited myocardial fibrosis^{130,131}. This work is especially meaningful considering the similarities between the porcine and human hearts¹³².

Additionally, Ceccato et al. findings in a cell culture model in which cardiomyocytes were treated with conditioned medium from activated CFs (rich in cytokines and growth factors) ultimately leading to cardiomyocyte hypertrophy and believed to be the result of IGF1 signaling¹³³, depict a clear picture of CF importance in the cardiomyocyte development and function, with particular emphasis on the role of IGF1.

Lastly, McDevitt et al. found, through the incorporation of BrdU, that IGF1 mediated the *in vitro* proliferation of embryonic stem cells-derived cardiomyocytes through IGF1R¹³⁴. This was found both through the stimulation of cells with IGF1 enriched media and by the blockage of its receptor¹³⁴. However, due to the inability to distinguish between binucleation and cell division in cardiomyocyte⁷⁹, questions remain whether the IGF1 does, in fact, lead to hyperplastic or hypertrophic growth.

Overall, there is a broad consensus that IGF1 has a positive role in the cardiac response to ischemic injury through its effect on cardiomyocytes.

IGF1 effects on Cardiac Fibroblasts

IGF1 has been reported to lead to fibroblast activation through upregulation of *Acta2* and *Col1a1* expression in mouse pulmonary fibrosis model mediated by IGF1R¹³⁵. Regardless of the aforementioned fact and the known actions of IGF1 in cardiomyocytes (see above), our understanding of the role of IGF1 in CFs remains meager.

Reiss et al. showed in CFs obtained from fetal and neonatal mice that IGF1R is essential for fibroblast proliferation during myocardial development through BrdU incorporation¹³⁶. Plus, Diaz-Araya et al. using a primary CF cell culture model isolated from fetal, neonatal, and adult rats, showed that treatment with IGF1 resulted in a substantial increase in the production of ECM proteins, namely collagen type I, laminin, and fibronectin in CF from adult animals, characteristic of activated fibroblasts while little to no effect was observed in neonatal CF. This work suggests that IGF1 is a CF gene expression modulator and the response of CF to this growth factor is age-dependent, becoming more pronounced with time¹³⁷.

The previous results in adult CFs were corroborated with Li et al. experiments demonstrating that IGF1R signaling is responsible for α -SMA, collagen I, and metalloproteinases in a diabetic mouse model¹³⁸, however conclusive evidence of CF activation was not provided. In this regard, Daian et al.'s experiments in keloid fibroblasts found that IGF1 alone could not activate fibroblasts. However, the latter also found that cells treated with both IGF1 and TGF- β 1 had a more pronounced activation profile than cells treated with TGF- β 1 alone, suggesting a synergetic effect of IGF1 and TGF- β 1¹³⁹.

Diverging from the previous studies, but within the breadth of the positive role of IGF1 in the heart, Ock et al. found that treatment with IGF1 prevented cardiac fibrosis induced by the angiotensin II and found that the IGF1R mediated this effect¹⁴⁰.

Besides the former study, an elegant experiment by Takeda et al. proved that in response to pressure overload in the cardiac setting, far from being a passive actor, CFs through their secretion of paracrine factors, namely IGF1, into the interstitial milieu were key mediators of myocardial hypertrophy and adaptive responses in the heart¹⁴¹. With IGF1 playing an important protective role against pressure overload by inducing cardiomyocytes hypertrophy¹⁴¹. Plus, it was also shown that IGF1 could induce proliferation of cardiac fibroblasts, suggesting both a paracrine and autocrine action for IGF1¹⁴¹. This

study, therefore, indicates that CFs, through IGF1, are key effectors in the cardiac hypertrophy and remodeling of the cardiac tissue¹⁴¹.

All in all, the regenerative capacity of the neonatal heart has sparked intense study by the scientific community however, our understanding of the role of CFs in this transition remains meager. This is especially concerning given that the existing scientific literature reveals that CFs' secreted mediators, particularly IGF1, are critical effectors in modulating the surrounding ECM and cardiomyocyte growth. Therefore, this thesis aims at closing the gap in our understanding of this transition period.

Objectives

The main objective of this dissertation is to unveil the role of IGF1 on the mechanisms underlying cardiac regeneration and repair, particularly through its activity on CFs. To achieve this goal, we propose to:

- Characterize the expression of IGF1 and other IGF family proteins in mice at different stages of development (embryonic, neonatal, and adult)
- Investigate how the IGF1 expression varies in response to injury in both an adult (reparative period) and a neonate (regenerative period) mouse model of MI.
- Explore the role of IGF1 in fibroblast activation using mouse and human cardiac fibroblasts and accessing the expression of activation associated genes.
- Assess the protective role of IGF1 on cardiac fibroblasts, *in vitro*, upon hypoxic stress.

Materials and Methods

Animal model and ethical statement

Animal experiments were performed in accordance with i3S (Instituto de Investigação e Inovação em Saúde) Animal Ethics Committee and with DGAV (Direção Geral de Alimentação e Veterinária). Humane endpoints were followed according to the OECD Guidance Document on the Recognition, Assessment, and Use of Clinical Signs as Humane Endpoints for Experimental Animals Used in Safety Evaluation. C57BL/6 strain of mice was used as an animal model in this study.

Targeted Transcriptome Sequencing

Total RNA from embryonic day 16 (E16), postnatal (P) day 1 (P1), P3 and P7 mouse ventricles (n=3 for all groups) was isolated using the RNeasy Plus Mini Kit (QIAGEN). High integrity RNA was used to conduct the microarray-based Targeted Sequencing Analysis. Results were analyzed on Transcriptome Analysis Console (ThermoFischer Scientific), and only genes with a fold change $> \pm 2$ and False Discovery Rate (FDR) p -value < 0.05 were considered to be differentially expressed between groups. Heatmaps were prepared using the Average Linkage Clustering Method and Spearman Rank Correlation distance measurement. Gene ontology and KEGG pathways were analyzed using Enrichr.

Myocardial Infarction by permanent ligation model in adult mice

8-weeks old female C57BL/6 mice were weighed and injected with buprenorphine (0.08 mg/kg; Richter Pharma) intraperitoneally (IP) for analgesia purposes 20 min before anesthesia. Next, the mice were anesthetized by IP injection of Ketamine (75 mg/kg; Clorketam; Vetoquinol) and Medetomidine (1 mg/kg, Sededorm; ProdivetZN). The mice were hydrated by subcutaneous injection with 1 mL of saline with glucose solution, and their eyes were protected with lubricant. The intervention area hair was removed. The mice were put on the surgical table, over and under the stereomicroscope (Olympus SZX 10; Olympus) and disinfected with alcohol and povidone-iodine solution, three times alternating. Mechanical ventilation was initiated using a small-animal respirator (Minivent 845) coupled with an endotracheal tube. Next, a left thoracotomy was commenced on the third intercostal space, exposing the heart. Then the pericardial sac was removed. The first portion of the left anterior descending (LAD) artery was permanently ligated by passing a non-absorbable 7/0 suture (Silkam; B.Braun) under the artery and then knotting, thereby permanently occluding the vessel. Next, the intercoastal incision was closed using an absorbable 6.0 suture (Safil, B.Braun), followed by closing the skin incision using surgical staples. Next, anesthesia was reverted by IP injection of atipamezole

(5 mg/Kg; Reverter; Virbac). After re-establishing the respiratory, the mice were removed from assisted ventilation and recovered over a warming pad. After gaining the capacity to move, the animals were returned to the cage (over a warming bed) and given hydrated food pellets. Sham-operated animals underwent the same procedure except for LAD artery ligation. After this, analgesia and fluid therapy by injection of buprenorphine (0.08 mg/kg; Bupaq, Richter Pharma) and subcutaneous injection of 1mL of glycosylated saline were maintained every 12 hours up to 72 hours after surgery or until full recovery. Animals were euthanized by cervical dislocation 96h after surgery, and the hearts were harvested and processed for RNA extraction and western blot analysis. Heart tissue was collected from two zones of the myocardium: the infarct zone (IZ) located in the apical region of the heart in the animals subjected to MI and from the correspondent location in the sham-operated animals; and from a remote zone (RZ) located in the basal region as controls.

Myocardial Infarction by permanent ligation model in neonatal mice

Timed pregnancies were generated after overnight mating. The following morning, females with vaginal plugs were considered to be at E0.5. 1-day-old (first 24h of life, P1). C57BL/6 neonate mice were anesthetized by hypothermia for approximately 3 minutes until paw withdrawal reflex and cardiorespiratory movements ceased. Animals were laid in a supine position, and immobilization of the four limbs was done with adhesive tape on a cooled surface of the stereomicroscope Leica S8APO. An incision was made in the chest cavity between the 3rd and 4th ribs, and the left anterior descending (LAD) coronary artery was localized. Myocardial Infarction (MI) was induced by permanent ligation of this artery, with a non-absorbable 10/0 Dafilon® suture (B. Braun). Subsequently, the musculoskeletal thorax and the skin were sutured with a 7/0 Silkam® suture (B. Braun), and mice were exposed to the heat produced by a red-light lamp to revert anesthesia. Sham-operated animals experienced the same procedure up until the ligation of the LAD coronary artery. After confirmation of spontaneous breathing, the mice were marked with ink diluted in saline solution (0,9% NaCl), and annotations about the surgery were made about each animal. After operating all animals from the same litter, neonates were returned to the progenitor. To ensure analgesia in pups during and after surgery through nursing, paracetamol was placed in the water bottle (1.32 mg/mL) provided for the mother one day before birth and kept for four days.

Animals were weighed and euthanized at 3, 5 and 7days post-injury (dpi). Chest cavity was opened to expose the heart, and an injection of 4 mM KCl was performed to stop the heart in relaxation. Afterward, hearts were harvested and washed in Phosphate buffered solution (PBS). If needed, removal of extra tissue or vessels was performed, and the hearts were weighted.

Images of the hearts were acquired using a stereomicroscope Olympus SZX10 with an Olympus EP50 color camera. For histology, the hearts collected at 1 dpi were paraffin embedded as previously

described in Sampaio-Pinto et al., 2018. Briefly, the hearts were fixed in 10% formalin neutral buffer overnight for less than 16 hours at room temperature. Subsequently, hearts were processed for 13 hours in an automated processor (paraffin tissue processor Microm STP 120) through successive bath washes of 1 hour in PBS, increasing series of alcohols (70%, 80%, 90%, 95%, 3x 100%), 3x Clear Rite 3[®] (Richard-Allan Scientific) and 2x paraffin. Hearts were oriented with the ventral side facing the bottom of the mold and included in paraffin using modular embedding system Microm STP 120-1. Leica RM2255 microtome was used to cut longitudinal sections with 3 μ m of thickness and cut up to the central region of the heart. Sections were finally placed in an incubator at 37°C overnight and then stored at 4°C.

For RNA isolation, hearts collected at 3, 5, and 7 days-post surgery were harvested and cleaned, then were divided into ventricles (bottom 2/3 of the heart) and atria (top 1/3 of the heart), and snap frozen in dry ice inside eppendorfs, and stored at -80°C.

Histology Masson trichrome

Masson Trichrome staining was performed using the Trichrome Stain (Masson) Kit (Sigma-Aldrich, HT15) in heart sections. Paraffin sections were placed at room temperature for 30 minutes and dewaxed as described in Sampaio-Pinto et al., 2018. After having dried, sections were mounted with Entellan mounting medium and a 0.13 mm glass coverslip. Sections were stored at room temperature. Whole heart section images were acquired with an Olympus SZX10 stereomicroscope with an Olympus EP50 color camera. High magnification images (100x) were acquired with the inverted fluorescence microscope Axiovert 200M and an AxioCam HRm camera (Zeiss), and the images were analyzed with Fiji software.

Cell Culture

Adult C56BL/6 mouse cardiac fibroblasts (mCF) were isolated from a single cell suspension which was obtained according to an adapted protocol of the gentleMACS™ Tissue Dissociator (Miltenyi Biotec). Briefly, 6-to-12-week mouse hearts were mechanically and enzymatically digested. The resulting cell suspension was left to adhere onto a tissue culture plate and removed 2 hours later to promote fibroblasts' selective adhesion. Fibroblasts were further expanded in Claycomb medium (Sigma Aldrich #51800C) supplemented with 10% Fetal Bovine Serum (FBS) (Lonza #DE14-801F), 1% L-glutamine (Gibco #25030-24) and 1% Pen/Strep.

Primary human cardiac fibroblasts (HCF) (Sigma #306-05A) were maintained and expanded in Fibroblast Growth Medium (FGM) (Cell Applications #316-500) at 37°C and 5% CO₂ until confluence. Cells (mCF and HCF) were dissociated with trypsin for cell passage, seeding, or freezing. And counted using a hemacytometer.

Cardiac fibroblasts activation assays

A cardiac fibroblast activation protocol using TGF- β 1 has been previously established in the group. Briefly, for CF activation with TGF- β 1, cells were seeded at a density of 8000 cells/cm² (mCF) or 36500 cells/cm² (HCF) in high glucose- Dulbecco's Modified Eagle Medium (DMEM) (Gibco #41965-039) supplemented with 10% FBS, 1% Penicillin/Streptavidin (P/S) and 0.2 mM ascorbate-2-phosphate (Asc 2-P, Sigma #49752) and incubated at 37°C 5% CO₂ for 24h. (Day -3). The cells were starved by changing the medium to high glucose-DMEM supplemented with 0.1% FBS, 1% P/S, and 0.2 mM Asc 2-P from day -2 onwards and were treated with TGF- β 1 5 ng/mL (mCF) or 10 ng/mL (HCF) (Peprotech #100-21). 3 days after seeding and every second day after that.

To assess the effect of IGF1 on human cardiac fibroblast activation, HCFs were adapted the activation protocol exchanging TGF- β 1 for IGF1 (Novus Biologics #NBP2-35000) at 0.1; 1 or 10 μ g/mL. Untreated cells and cells treated with TGF- β 1 (10 ng/mL) were used as negative and positive controls of fibroblast activation, respectively. HCF activation was assessed at different time points (from D0 to D7) by assessing the expression of genes associated with cardiac fibroblast activation.

RNA isolation

RNA was extracted from mice heart tissue from Sham and MI animals collected 24h, 48h, or 96h post-injury in adult mice and 3, 5, and 7 days post-injury in neonatal mice. The tissue was homogenized in QIAzol Lysis Reagent (Qiagen #79306) using a tissue homogenizer (IKA Ultra-Turrax). RNeasy® Plus Mini Kit (Qiagen #1038703) was used to purify total RNA while ensuring the removal of genomic DNA, according to manufacturer instructions.

For RNA extraction from cells, the cells were lysed with QIAzol Lysis Reagent (Qiagen #79306) according to the manufacturer's instructions and kept at -80°C until further use. Briefly, cell extracts were vortexed and incubated for 5 min at RT. Then 0.2 mL of Chloroform (Sigma-Aldrich #496189-1L) was added per 1mL of initial QIAzol Lysis Reagent used. The samples were then capped and shook vigorously for 15 s, incubated at room temperature (RT) for 3 min, and centrifuged at 12000g for 15 min at 4°C. The aqueous phase (where the RNA remained) was transferred to a fresh RNAase-free tube. The RNA was precipitated by adding 250 μ L of isopropanol (Thermo Fisher Scientific #327270010) per 500 μ L of QIAzol used plus 1 μ L glycogen (20 mg/mL, Thermo Fisher Scientific #R0561) to increase the precipitation recovery of RNA. Next, the tubes were vortexed and placed at -20 °C overnight. The following day, the samples were centrifuged at 12000g for 30 min at 4°C, the supernatant was removed, and the RNA pellet was washed twice with 1 mL of 75% RNase-free ethanol (Merk Millipore #100983) per 500 μ l of initial QIAzol used. followed by centrifugation at 7500g for 5 min at 4°C. After the last wash the ethanol was removed, and the RNA left to air-dry. The RNA

pellet was then resuspended in 10-15 μ L of RNase-free water (Qiagen #129112) and RNA concentration and quality determined using Nanodrop 1000 spectrophotometer (Thermo Fisher Scientific).

Real-Time qPCR

Reverse transcription was performed to synthesize complementary DNA using PrimeScript RT Enzyme Mix (Takara Bio #RR037A-2) according to manufacturer instructions. Real-time Polymerase Chain Reaction (qRT-PCR) was performed in CFX96 Touch Real-Time PCR Detection System (Bio-Rad) using iTaq™ SYBR Green supermix (Bio-Rad #1725120). Primer sequences are specified in Table 1 and the PCR cycles are indicated in Table 2. Gene expression was calculated using the difference between the mean threshold cycle values between the reference (GAPDH) and the genes of interest ($2^{-\Delta Ct}$ method).

Table 1 - Primer sequences for qRT-PCR

| Gene | Primer sequence (5' to 3') | PCR product length | Annealing Temperature (°C) |
|---------|---|--------------------|----------------------------|
| mIGF1 | FW: CACACCTCTTCTACCTGGCG RV: GTACTTCCTTCTGAGTCTTGGGC | 321 bp | 60 |
| mIGF2 | FW: GTGCTGCATCGCTGCTTAC RV: ACGTCCCTCTCGGACTTGG | 222 bp | 60 |
| mIGFBP1 | FW: ATCGCCGACCTCAAGAAATGG RV: AGAGTCCAGCTTCTCCATCCA | 187 bp | 60 |
| mIGFBP2 | FW: CCCAGACGCTACGCTGCTAT RV: CCTCCCTCAGAGTGGTTCGTC | 145 bp | 60 |
| mIGFBP3 | FW: GCAGCCTAAGCACCTACCTC RV: CTTGGAATCGGTCACTCGGT | 128 bp | 60 |
| mIGFBP4 | FW: TGTCGGAAATCGAAGCCATCC RV: AGGGGTTGAAGCTGTTGTTG | 84 bp | 60 |
| mIGFBP5 | FW: CAACGAAAAGAGCTACGGCG RV: ACCTTGGGGGAGTAGGTCTC | 105 bp | 60 |
| mIGFBP6 | FW: CAACCCCGAGAGAACGAAGAG | 167 bp | 60 |

| | | | |
|------------------|---|--------|----|
| | RV: CGTGGATTCTTCTGCCGGTC | | |
| mIGFBP7 | FW: TGCGAGCAAGGTCCTTCCATA RV: CGCTGAACTCCAGAGTGATCC | 149 bp | 60 |
| mHTRA1 | FW: AGTCACCACTGGGATCGTCA RV: AATCCCAATCACCTCGCCAT | 154 bp | 60 |
| hACTA2 | FW: GGCAAGTGATCACCATCGGA RV: GTGGTTTCATGGATGCCAGC | 100 bp | 60 |
| hCol1 α 1 | FW: GAGGGCCAAGACGAAGACA RV: CAGATCACGTCATCGCACAAC | 140 bp | 60 |
| hCol3 α 1 | FW: GGAGCTGGCTACTTCTCGC RV: GGGAACATCCTCCTTCAACAG | 78 bp | 60 |
| hCTGF | FW: CTTGCGAAGCTGACCTGGAAGA RV: CCGTCGGTACATACTCCACAGA | 148 bp | 60 |
| hFAP | FW: TCTGGAAAAATGAAGACTTGGGT RV: CAGTGTGAGTGCTCTCATTGTA | 141 bp | 60 |
| hIGF1 | FW: CTTCAGTTCGTGTGTGGAGAC RV: GGTAGAAGAGATGCGAGGAGG | 128 bp | 60 |

Table 2 - qRT-PCR cycling conditions

| Cycle | # Cycles | Step | Time | Temperature (°C) |
|-------|----------|---------------|------------|------------------|
| 1 | 1 | Activation | 3min 30sec | 95 |
| 2 | 40 | Denaturation | 20 sec | 95 |
| | | Annealing | 30 sec | 60 |
| 3 | 81 | Melting Curve | 10 sec | 55 |

Immunofluorescence

For the immunofluorescence assay, HCF were seeded in 96 well Perkin Elmer Cell Carrier Ultra plates at a density of 36500 cells/cm² and underwent an activation protocol as described above. On day 6

of the activation assay, the cell media was removed, and the cells were fixed with 4% paraformaldehyde (PFA) in PBS for 15 min at RT. The PFA was removed, and the cells were washed twice with PBS for 3 min and kept at 4°C until further use. The cells were then permeabilized with 0.1% Triton-X100 in PBS for 10 min at RT. Next, the cells were washed 2 times with PBS for 3 min and blocked with 1% BSA plus 4% FBS in PBS-T (PBS plus 0.05% Tween[®]-20 for 1h at RT. Cells were then incubated with mouse anti- α -smooth muscle actin (α -SMA) primary antibody (Sigma-Aldrich #A5228) at 1:250 dilution in blocking solution overnight at 4°C. The next day, the cells were washed 3 times with PBS-T for 3 min, followed by incubation with donkey anti-mouse Alexa Flour 594 (Thermo fisher #A21203) secondary antibody at 1:1000 in blocking solution for 2h at RT. The cells were washed 3 times with PBS-T for 3 min and stained with Phalloidin 488 (Santa Cruz Biotechnologies #363791) at 1:500 in PBS for 20 min at RT. Again, the cells were washed 3 times with PBS-T for 3 min, and the nuclei were stained with 1 μ g/mL 4,6-diamidino-2-phenylindole (DAPI) for 5 min at RT and washed 2 times with PBS. The cells were kept in PBS protected from light at 4°C until image acquisition using an INCell Analyzer 2000 (GE Healthcare Life Sciences, USA) with Nikon 20X/0.45 NA Plan Fluor objective and the 4,6-diamidino-2-phenylindole (DAPI), Texas Red and FITC filters. The number of cells per field of view (FOV) was counted using Fiji software (ImageJ version 1.51j, NIH, USA)¹⁴².

Survival Assay

Human CFs were seeded at 36500 cells/cm² in 24-well plates with coverslips in high glucose-DMEM supplemented with 10% FBS, 1% P/S, and 0.2 mM Asc 2-P until cell adhesion (aprox. 6h) at 37°C and 5% CO₂. Then the cells were starved by changing the medium into high glucose-DMEM supplemented with 0.1% FBS, 1% P/S, and 0.2 mM Asc 2-P in the presence of 0, 0.1, 1, or 10 μ g/mL IGF1, in triplicate. The cells were then transferred into a hypoxia chamber (1% O₂) at 37°C and incubated for 72h. In parallel, cells were kept under normoxia conditions as a control. After 72h, cells were fixed with 4% PFA in PBS for 15 min at RT washed, and apoptosis induced by the hypoxic stress was assessed by a TUNEL assay (Tdt-mediated dUTP nick-end labeling) using the Apoptag[®] fluorescein in situ apoptosis detection kit (Merk Millipore #S7110) according to the manufacturer's instructions. Counterstaining was performed with 1 μ g/mL of DAPI in PBS for 5 min at RT. The coverslips were and mounted in a glass slide using Fluoroshield[™] mounting media (Sigma #F6182). Images were acquired using an Olympus BX53 fluorescence microscope (Hamburg, Germany) with the 10x objective. Image Analysis was performed with Fiji software (ImageJ version 1.53j, NIH, USA)¹⁴².

Western Blot

Heart tissue was dissociated in Radioimmunoprecipitation assay buffer (RIPA) supplemented with protease inhibitor cocktail (1:100, Sigma-Aldrich #P8340) using a PYREX® Potter-Elvehjem tissue grinder with mechanical force. The tissue extracts were kept on ice for 30 min to ensure cell lysis and centrifuged at 21000 g for 15 min at 4 °C to remove major tissue/cellular debris and the supernatant collected and stored at -80 °C.

Human cardiac fibroblasts were washed with PBS and lysed with RIPA buffer supplemented with protease inhibitor cocktail (1:100), and cell extracts were preserved at -80 °C until further use.

To ensure sample homogeneity, protein quantification was performed using the modified Lowry method (DC™ Protein Assay Kit II, Biorad #5000112) accordingly to the manufacturer's instructions. Absorbance at 750nm was read using a Synergy™ Mx Microplate Reader (BioTek). The samples (10-20 ug of protein) were boiled for 5 min at 95°C in SDS-PAGE loading buffer (50 mM Tris-HCl pH 6.8, 2% SDS, 0.05% bromophenol blue, 10% glycerol) and loaded into an 8% SDS-PAGE gel. Precision Plus Protein Dual Colour Standards (Biorad #1610374) ladder was used as a molecular weight marker. Next, the proteins were electroblotted into a nitrocellulose membrane (Amersham TM Protran TM 0.45 µm GE Healthcare Life science), using a semi-dry transfer system (Biorad #1703940) accordingly to the manufacturer's instructions. Transfer efficiency and protein loading was controlled using Ponceau Staining. The membrane was blocked with 5% BSA in Tris buffered solution (TBS) supplemented with 0.05% Tween®-20 (TBS-T) for 1h at RT and incubated with rabbit anti-IGF1Rβ primary antibody (Cell Signalling Technology #A3027) 1:500 in blocking solution at 4°C overnight. The membranes were then washed 3 times with TBS-T for 5 min and incubated with goat anti-rabbit secondary antibody conjugated with horseradish peroxidase (HRP) at 1:10000 (SBI EXOAB-HRP) in blocking solution for 1h at RT followed by 3 times wash with TBS-T. For the loading control, we used α-tubulin (for tissue extracts) or GAPDH (for cell extracts), which were detected by incubating the membranes with primary mouse anti-α-tubulin antibody 1:5000 (Santa Cruz Biotechnology, #sc-38035) or mouse anti-GAPDH 1:10000 (Santa Cruz Biotechnology, #sc-32233) in blocking solution for 1h at RT followed by goat anti-mouse HRP (Invitrogen #AP271) secondary antibody at 1:10000 in blocking solution for 1h RT. Immunoreactive bands were revealed by chemiluminescence using Clarity™ Western ECL substrate (Biorad #170-5061) and Bio-Rad ChemiDoc™ XRS+ Imager (Biorad). Blots were quantified by densitometry analysis using Fiji software. Loading correction was achieved by dividing the density of the IGF1Rβ band by the respective density of tubulin or GAPDH.

Data and statistical analysis

Statistical testing was performed using GraphPad® Prism 7.0 Software. The normality of the data was assessed through the Shapiro-Wilk test. In the data that passed the normality test (Figure. 2F, 3C, 4C, 6B, 6D, 7B, S1 and S3), statistical significance was tested by One-way ANOVA. The p values for individual comparisons were calculated using Tukey's test. In Figure 3D, statistical significance was tested by Two-way ANOVA and p values for individual comparisons calculated by Bonferroni's test. In the data that did not pass the normality test (Figure 5B (right panel) and S4), statistical significance was tested by non-parametric One-way ANOVA Kruskal-Wallis test, and p values for individual comparisons were calculated using Dunn's test. Results are presented as mean \pm SD, and differences between groups were considered significant when $p < 0.05$.

Results

***Igf1* and *Igf2* are differently expressed during the cardiac regeneration-repair transition**

Understanding the transcriptional alterations during the transition between cardiac regeneration and repair is of utmost importance to identify key mechanisms regulating these processes¹⁴³. To this end, we performed targeted RNA-sequencing of mouse ventricles at embryonic day 16 (E16) and postnatal days 1, 3, and 7 (P1, P3, and P7, respectively). Unsupervised hierarchical clustering of all samples showed a clear association of the three replicates from the same age group and the formation of two main clusters E16-P1 and P3-P7 (Figure 2A). The clustering of samples by age group is found in the principal component analysis (PCA) plot (Figure 2B). The horizontal axis, which explains 33.3% of the differences between samples, indicates a progression of these differences with age, with the P7 group being more distant from E16 than any other group.

Regarding differentially expressed genes (DEG) between all possible pairwise comparisons, E16 vs P7 yielded the highest number (1665 genes) and P3 vs P7 the lowest number (442 genes) (Figure 2C). Then, we focused our analysis on the transcriptional alterations between a regenerative (P1) and reparative (P7) stage. Altered biological processes and pathways associated with DEG between P1 vs P7 showed cell cycle genes were downregulated in P7, while genes related to ECM and the matrisome were highly upregulated at P7 (Figure 2D). Gene ontology terms associated with DEG lists of all possible comparisons consistently showed altered ECM and ECM-related genes, indicating that the extracellular environment is severely remodeled around birth (data not shown). The IGF gene family was identified in a cross-referencing with known matrisome-associated genes^{144,145} because several family members were found differentially expressed with age (Figure 2E). Interestingly, not all IGF family members followed the same expression trend during this development window. For example, IGF2, IGFBP3, and IGFBP5 were downregulated at P3 and P7 when compared with E16 and P1, whereas IGF1, IGFBP7, and HTRA1 showed an inverse tendency.

To validate these RNAseq results, the same samples were subjected to qPCR for the genes *Igf1*, *Igf2*, and several IGF binding proteins (Figure 2F and Figure S1). In accordance with the RNAseq data, we found that *Igf1* expression was significantly lower before birth (E16) and on the first day after birth (P1), compared to P3 and P7, which correlates with the loss of regenerative ability and onset of the reparative period. Regarding *Igf2*, and in accordance with RNAseq results, we observed a statistically significant downregulation of *Igf2* right from E16 to P1 and a continuous lowering expression till P7. Overall, the data obtained from the RNAseq showed a differential expression of the IGF family in the regenerative and reparative transition. These results support that the IGF family,

particularly IGF1 and IGF2, may be involved in the complex signaling that underlies the transition from the regenerative to the reparative response to injury in neonatal mice.

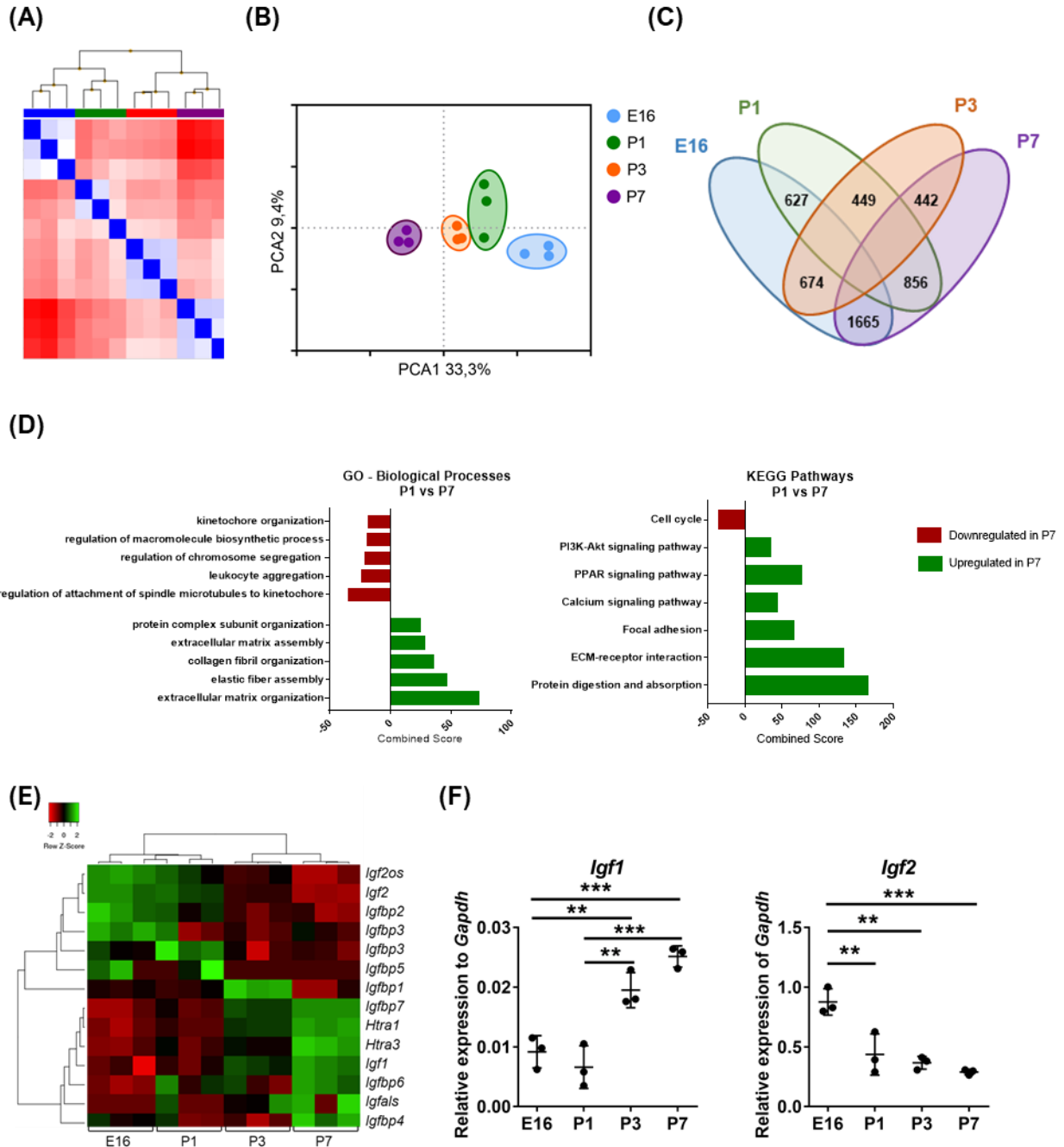


Figure 2 – *Igf1* and *Igf2* transcription is altered in the heart during the transition from regeneration to repair. (A-F) Targeted sequencing analysis of mouse heart samples at E16 (blue), P1 (green), P3 (orange) e P7 (purple). (A) Unsupervised hierarchical clustering and (B) PCA plot of RNAseq data. (C) Venn diagram of the number of differentially expressed genes (DEG) in each pairwise comparison. (D) GO and KEGG pathways enrichment analysis. (E) Heatmap of the differential expression of IGF family genes. (F) qPCR of *Igf1* (left) and *Igf2* (right) expression at E16, P1, P3, and P7 mice hearts. MI. Data was normalized to *Gapdh*, statistical significance was tested by One-way ANOVA, and *p* values for individual comparisons were calculated by Tukey's test. Values are mean ± SD, n=3, **p*<0.05; ***p*<0.01, ****p*<0.001.

***Igf1* expression is increased in mice after MI**

The differential expression of the IGF gene family during the transition from regenerative to reparative stages led us to question how these genes were regulated upon injury.

Our first approach was to evaluate the expression of *Igf1* and *Igf2* in heart samples already available at the lab. Samples were harvested from adult mice subjected to MI by surgical ligation of the left anterior descending (LAD) coronary artery at 24h, 48h, and 96h post-injury (Figure S2). Tissue samples were collected from the infarct zone, from a peripheral zone to the infarct, and from a remote heart zone, not directly affected by the MI. Sham-operated animals were used as controls. Although only one animal was analyzed per timepoint, these preliminary results indicate that *Igf1* and *Igf2* were upregulated 96h after injury in the infarct region.

We repeated the experiment with more animals as schematized in Figure 3A and collected the hearts 96h post-MI (n=4) to explore these preliminary results further. Tissue from the infarct zone, on the apical area of the left ventricle, and from a remote zone, on the basal area of the heart was collected. Sham (n=3) operated animals were used as controls. Post-MI, the expression of *Igf1*, *Igf2*, and the genes coding for other IGF-associated proteins, namely *Igfbp1-7* and *Htra1*, were assessed by qPCR (Figure 3C and S3). *Igf1* expression significantly increased in the infarct zone after MI compared with the remote region and sham-operated animals. Contrarily to *Igf1*, *Igf2* was not as evidently upregulated after MI in the infarct zone (Figure 3C).

Regarding the IGF associated proteins analyzed, *Igfbp3*, *Igfbp4*, and *Igfbp7* presented a similar expression response as *Igf1* to MI. *Igfbp6* and *Htra1* did not show significant alterations after injury, whereas *Igfbp5* showed a tendency for increased expression, however, not reaching statistical significance (Figure 3C). *Igfbp1* and *Igfbp2* expression (Figure S3) was very low, which raised questions about their transcripts' biological significance in the context of the heart.

Since IGF1R mediates IGF1 effects, we decided to assess the myocardial tissue levels of IGF1R by western blot, in which a significant decrease of IGF1R was found in the infarcted region compared with the remote region. No differences were observed in the sham-operated animals (Figure 3D).

Taking into consideration that *Igf1* was upregulated after MI in the adult mouse heart, and to explore the translational relevance of these findings, we assessed the IGF1 concentration in pericardial fluid and plasma samples collected from patients undergoing coronary artery bypass grafting, previously available in the laboratory, using an ELISA assay (Figure S4). The study included two groups of patients: a control group with stable angina and no history of the acute coronary syndrome and a MI group constituted by patients with a recent (<3 months) MI. The groups were similar in terms of age, sex, age, cardiovascular risk factors, and medication at the time of surgery (data not shown). Our results show that the IGF1 concentration was higher in the pericardial fluid of patients with MI compared with the control group, whereas no differences were detected in the plasma. These results were relegated to the supplementary data because the values obtained in the samples of interest were lower than those obtained for the assay standards.

Overall, these results suggest that the IGF1, together with IGF1R, which mediates its activity, are altered in response to ischemic injury in adult mice (reparative period).

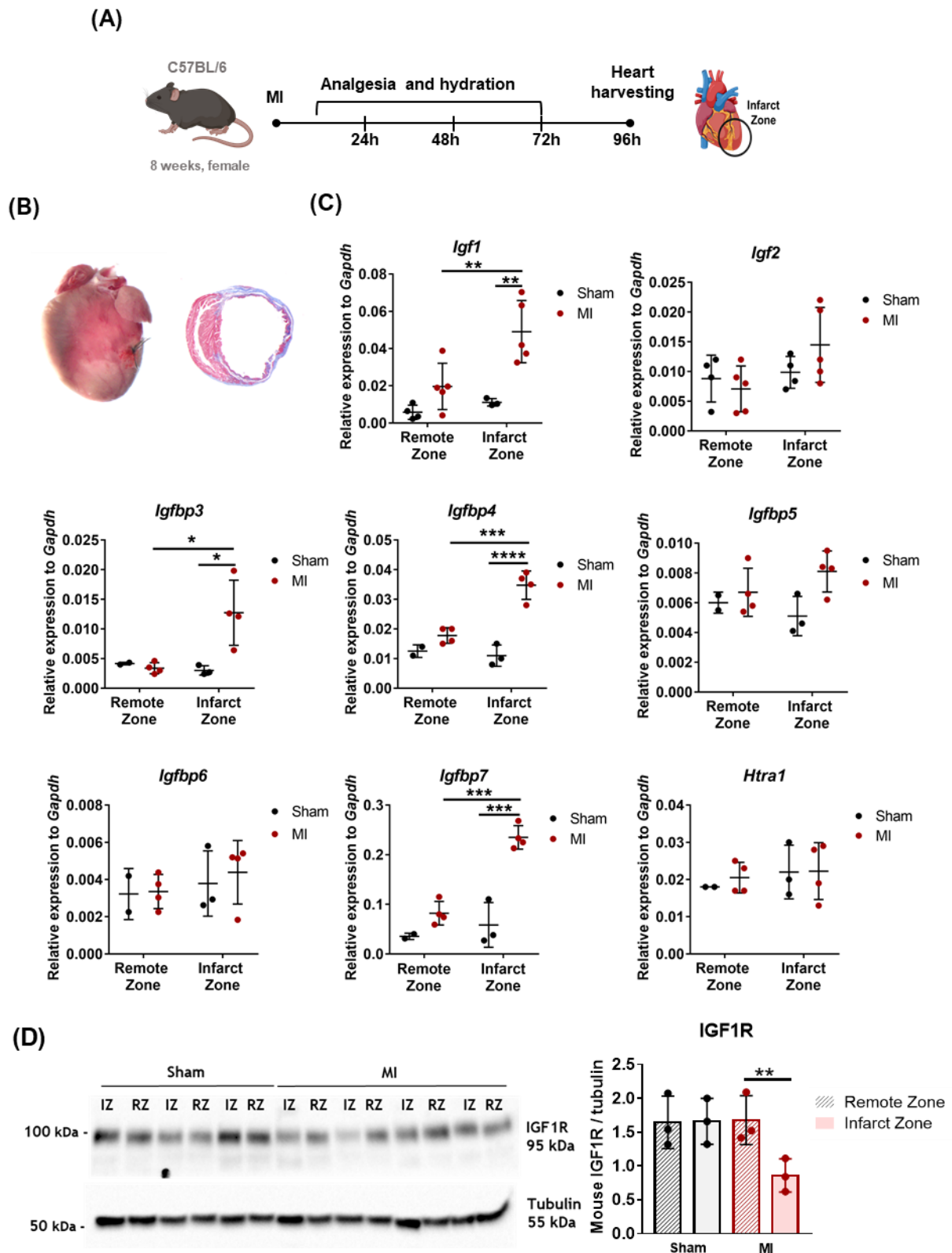


Figure 3 – IGF family is differently expressed after MI in adult mice. (A) Schematic representation of the MI model in adult mice. Representation of the infarct zone location in the heart. (B) Left, stereomicroscope representative image of a mouse infarcted heart 24h after surgery. Right, Masson's Trichrome staining of a

transversal section of a mice heart, collected 21 days after injury (MI). **(C)** qPCR of *Igf1*, *Igf2*, *Igfbp3*, *Igfbp4*, *Igfbp5*, *Igfbp6*, *Igfbp7*, *Htra1* expression in sham and MI animals 96h after MI. Data was normalized to *Gapdh*, statistical significance was tested by One-way ANOVA, and *p* values for individual comparisons were calculated by Tukey's test. Values are mean \pm SD, n=2-5 **p*<0.05; ***p*<0.01, ****p*<0.001, *****p*<0.0001. **(D)** Western blot (left) and respective quantification (right) of IGF1R in the infarct zone (IZ) and remote zone (RZ) of MI and sham-operated hearts. Data was normalized to α -tubulin, statistical significance was tested by Two-way ANOVA, and *p* values for individual comparisons were calculated by Bonferroni's test. Values are mean \pm SD, n=3.

***Igf1* and *Igf2* expression is decreased during neonatal heart regeneration**

Next, and with the transition between the regenerative and repair periods in mind, we evaluated the expression of *Igf1* and *Igf2* in the context of neonatal MI at P1, a period in which animals can mount an effective regenerative response (Figure 4A and 4B). Whole ventricles were harvested at 3, 5, and 7 days post-injury (dpi), and the expression of *Igf1* and *Igf2* was assessed by qPCR (Figure 4C). Sham-operated animals were used as controls. Differing from the results obtained in the transcriptomics of non-manipulated hearts from E16 to P7 (and subsequent qPCR validation) (Figure 2) in which *Igf1* expression increased through time, in the neonatal MI mouse model, there is a decrease of *Igf1* between dpi 3 and dpi 5 and having a modest (non-statistically significant) uptick at dpi 7 (Figure 4C, left panel). However, for *Igf2*, it was observed that both the sham and the MI hearts (Figure 4C, right panel) follow the same descending pattern as in the RNAseq data (Figure 2DE), not showing to be influenced by the injury. Both *Igf1* and *Igf2* were downregulated 3 days after MI compared to sham-operated controls. These findings contrast with the results obtained for the adult counterparts (Figure 3C), especially in what concerns *Igf1* expression, supporting a different role for IGF1 in response to MI between neonatal and adult periods.

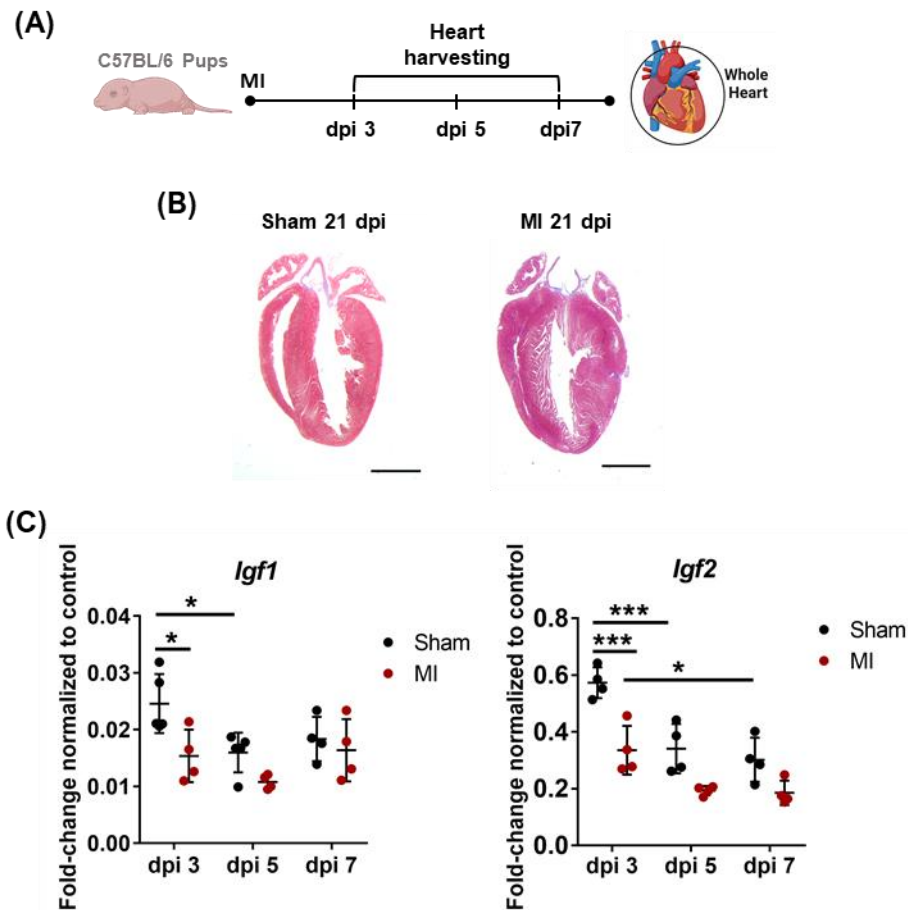


Figure 4 – *Igf1* and *Igf2* expression decreases with time after MI in neonatal (P1) mice. (A) Schematic representation of the MI model in neonatal mice. The whole heart was harvested at days 3, 5, and 7 post-injury. (B) Representative images of neonatal mice regenerative potential, collected 21 days after injury, following Masson's Trichrome stain. Sham surgery (left) or myocardial infarction performed at 1 day of life (right); Scale bar 2 mm (C) qPCR of *Igf1* and *Igf2* expression in sham and MI animals 3, 5 and 7 dpi. Data was normalized to *Gapdh*, statistical significance was tested using One-way ANOVA, and *p* values for individual comparisons were calculated by Tukey's test. Values are mean \pm SD, *n*=4, * *p*<0.05; ****p*<0.001.

IGF1 expression is increased during *in vitro* cardiac fibroblast activation

Cardiac fibroblasts have been shown to change their phenotype around birth and are involved in neonatal regeneration and adult-heart repair^{23,84}. In order to explore the role and the translational potential of CFs and IGF1 in regeneration and repair, a cardiac fibroblast activation protocol, *in vitro*, was used in both mouse and human CFs (mCFs and HCFs, respectively) (Figure 5A). CFs activation to myofibroblasts was accomplished by treating the cells with TGF- β 1 3 days after seeding and every second day after that, namely days 0, 2, 4, and 6. We observed that when treated with TGF- β 1, mouse and human CFs showed consistent upregulation of gene encoding IGF1, compared to untreated cells (Figure 5B), however, without attaining statistical significance. Also, no significant

variability was observed between the different activation timepoints. These results indicate that TGF- β 1-mediated cardiac fibroblast activation induces the expression of the IGF1 genes in both mouse and human cells.

Besides the increase in the expression of the genes coding for IGF1, we also asked if TGF- β 1-mediated CFs activation alters the levels of the IGF1R, and we assessed that by western blot in HCFs (Figure 5C). When treated with TGF- β 1, HCFs show an increased IGF1R on day 4 of activation compared with the non-activated cells, whereas on day 6, this pattern reverses, and the untreated condition revealed higher protein levels than the one treated with TGF- β 1. These results will require further investigation since they were obtained from only two independent experiments and present a considerable high standard deviation.

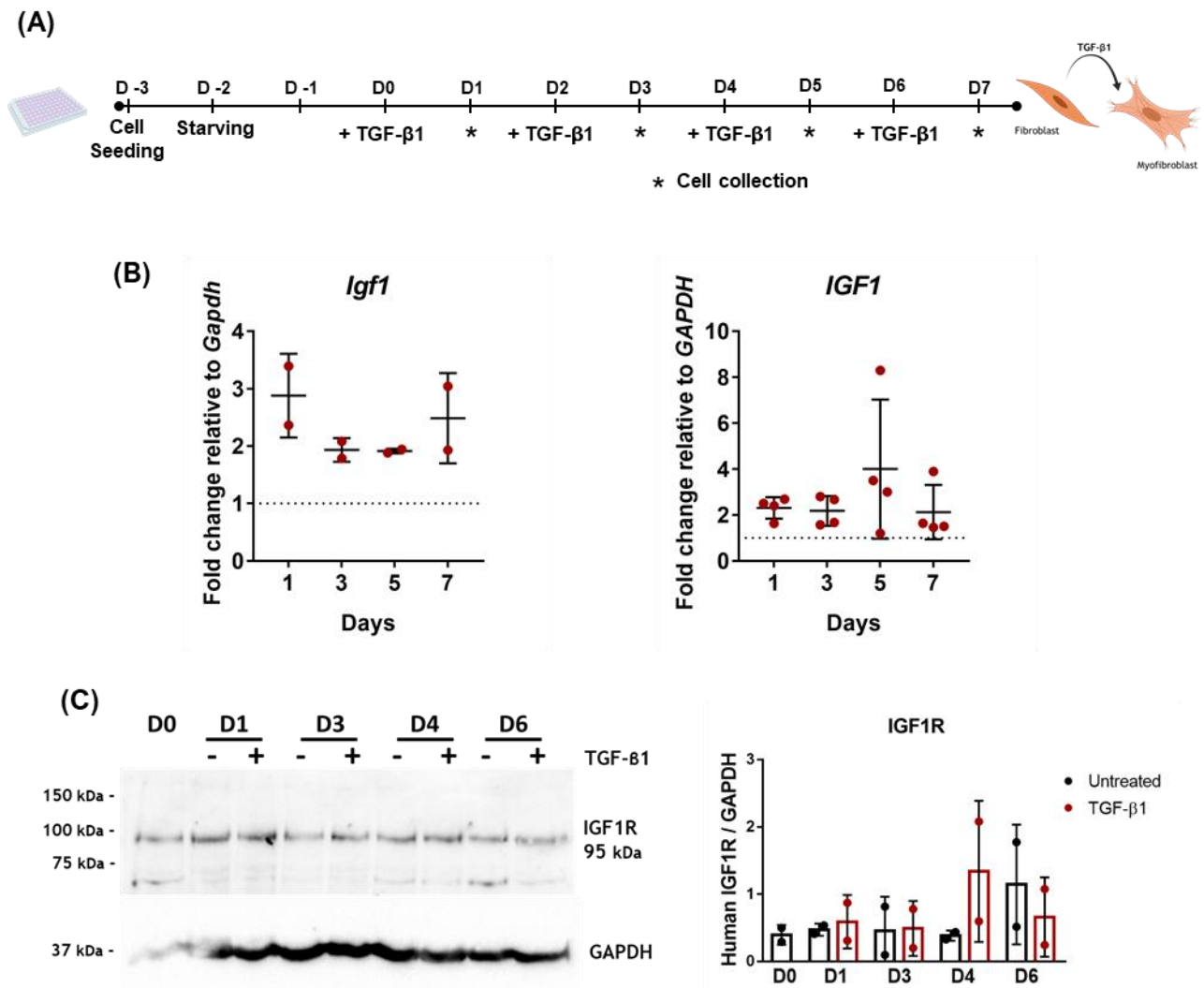


Figure 5 – IGF1 expression is increased in activated cardiac fibroblasts. (A) Schematic representation of CFs activation protocol **(B)** Fold change on IGF1 expression after TGF- β 1 stimulation of mCF (left, n=2) and HCF (right, n=4) and untreated cells of the same day (dotted line at Y=1). Statistical analysis was tested by non-parametric One-way ANOVA through Kruskal-Wallis analysis followed by Dunn's test. No statistically significant changes were found between the fold changes of different timepoints on HCFs (right panel). Values are mean \pm SD **(C)** Determination of IGF1R in HCF treated or not with TGF- β 1 through time. Left panel, western blot (representative blot of two independent experiments) of IGF1R. Right panel, quantification of IGF1R normalized for GAPDH. Values are mean \pm SD, n=2.

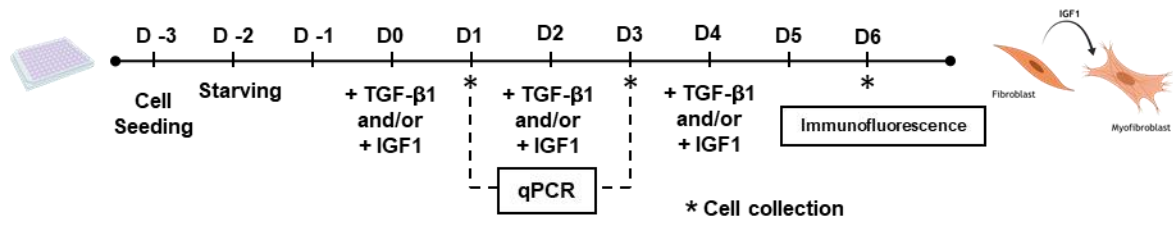
IGF1 role on human cardiac fibroblast activation

To assess if IGF1 is implicated in fibroblast activation *in vitro*, we challenged HCFs with growing concentrations of IGF1 (0.1 – 10 μ g/mL) and assessed the expression of genes associated with fibroblast activation by qPCR (Figure 6A and 6B). As a positive control, HCFs were treated with TGF- β 1. We observed increased transcription of α -SMA, Collagen I, CTGF, and FAP coding genes compared with the untreated cells (Figure 6B). However, this observed tendency was not statistically significant. We also observed that the increased expression of the activation markers with IGF1 was not dose-dependent.

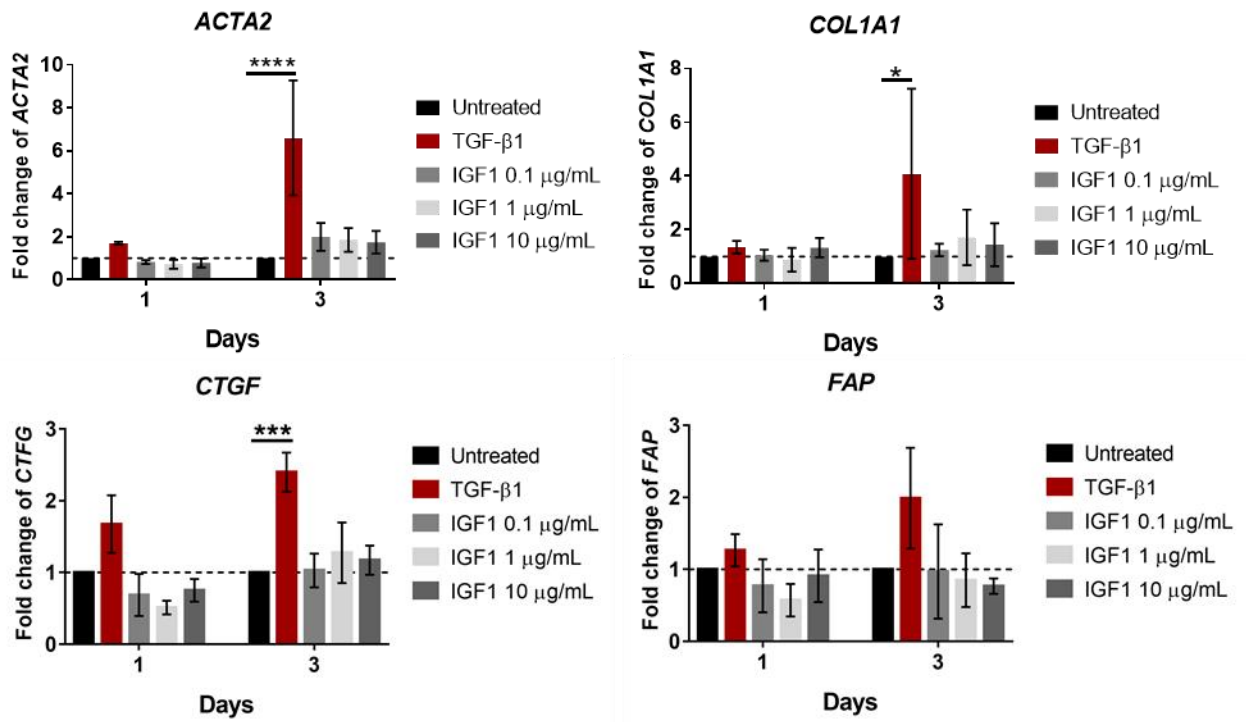
Following the qPCR results, we decided to examine the accumulation of α -SMA, a marker of activated cardiac fibroblasts, in HCF treated with the highest IGF1 concentration (10 μ g/ml) at day 6, by immunofluorescence (Figure 6A and 6C). The results show that despite no significant increase in *ACTA2* expression after 6 days of treatment with IGF1, there is a statistically significant increase in the number of α -SMA⁺ CFs, compared with the untreated cells, although not as marked as following TGF- β 1 stimulation (Figure 6C). Also, no synergistic effect of IGF1 and TGF- β 1 treatment in the number of HCF activated was found.

Overall, our results indicate that IGF1 is able to induce HCF activation *in vitro*.

(A)



(B)



(C)

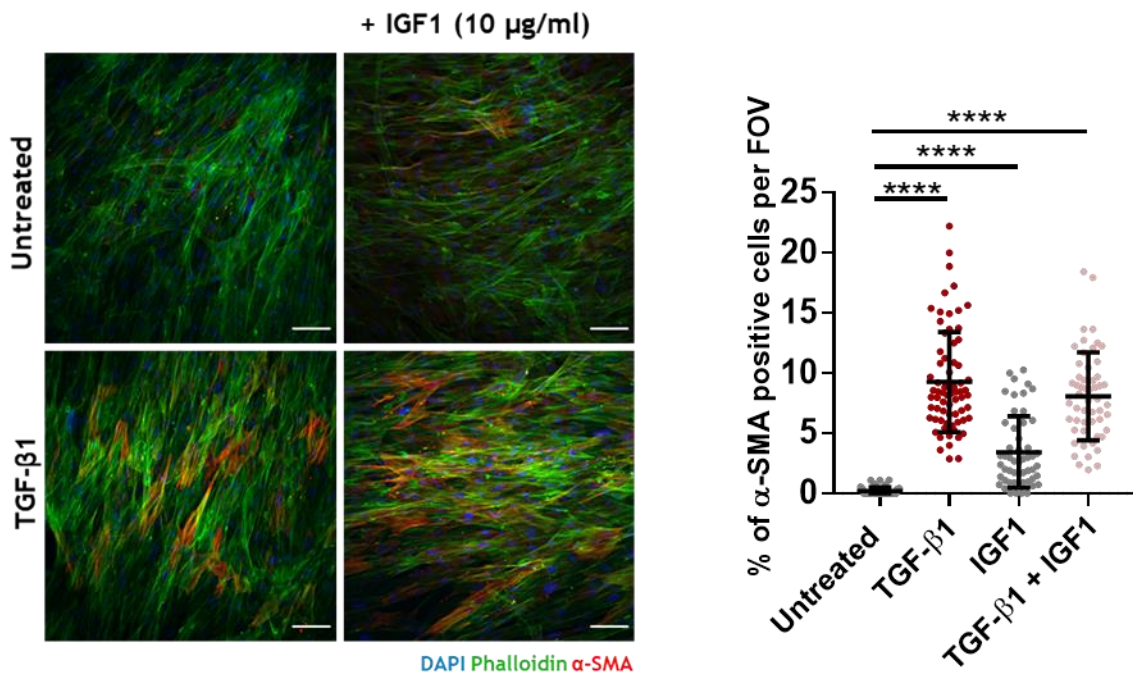


Figure 6 – IGF1 is able to induce HCF activation. (A) Schematic representation of the adapted CF activation protocol (B) Fold change expression of the activation markers *ACTA2*, *COL1A1*, *CTGF*, and *FAP* in HCF treated with growing concentrations of IGF1 (0.1, 1, 10 $\mu\text{g}/\text{mL}$), relative to untreated cells of the same day (dotted line at $Y=1$). TGF- β 1 (10 ng/mL) was used as a positive control of activation. Data was normalized to *GAPDH*, and statistical significance was tested by One-way ANOVA, and p values for individual comparisons were calculated by Tukey's test. Values are mean \pm SD, $n=3$ * $p<0.05$; *** $p<0.001$, **** $p<0.0001$. (C) Quantification of α -SMA positive HCF upon treatment with IGF1 for 6 days. Left panel, representative images (two independent experiments) of HCF treated with 10 ng/mL TGF- β 1 and/or 10 $\mu\text{g}/\text{mL}$ IGF1. Cells were immunolabeled for α -SMA (red), phalloidin (green) was used as a cytoplasm marker, and the nuclei were stained with DAPI (blue). Scale bar=100 μm . Right panel, quantification of the percentage of α -SMA positive cells per field of view (FOV), at least 700 cells were counted per condition using Fiji software. The total amount of cells was achieved by counting cell nuclei. Activated cells (α -SMA positive) were counted manually and divided by the total amount of cells. Statistical significance was tested by One-way ANOVA, and p values for individual comparisons were calculated by Tukey's test. Values are mean \pm SD, $n=2$, **** $p<0.0001$.

IGF1 has a protective effect against hypoxia-induced apoptosis in human CFs

IGF1 has been described as involved in cell survival and proliferation pathways¹²⁰ in cardiomyocytes and lung fibroblasts^{134,135,146}. Knowing that *Igf1* is upregulated after MI, it was hypothesized if IGF1 could also have a protective role in response to an ischemic injury.

To investigate IGF1's protective potential against cell death, we established an *in vitro* survival protocol where we subjected HCFs to hypoxic conditions (1% O₂ for 72h) in the presence or absence of IGF1 (0.1, 1 and 10 µg/mL) and assessed the levels of hypoxia-induced apoptosis using a TUNEL assay (Figure 7A and 7B). Cells maintained under normoxic conditions were used as controls. We observed that IGF1 was able to significantly protect HCFs from hypoxia-induced apoptosis, independently of the dose used (Figure 7B), rescuing the apoptosis levels observed in control cells.

This result suggests that IGF1 can be involved in response to ischemic injury in the context of MI by promoting CFs survival and contributing to the repairing mechanisms.

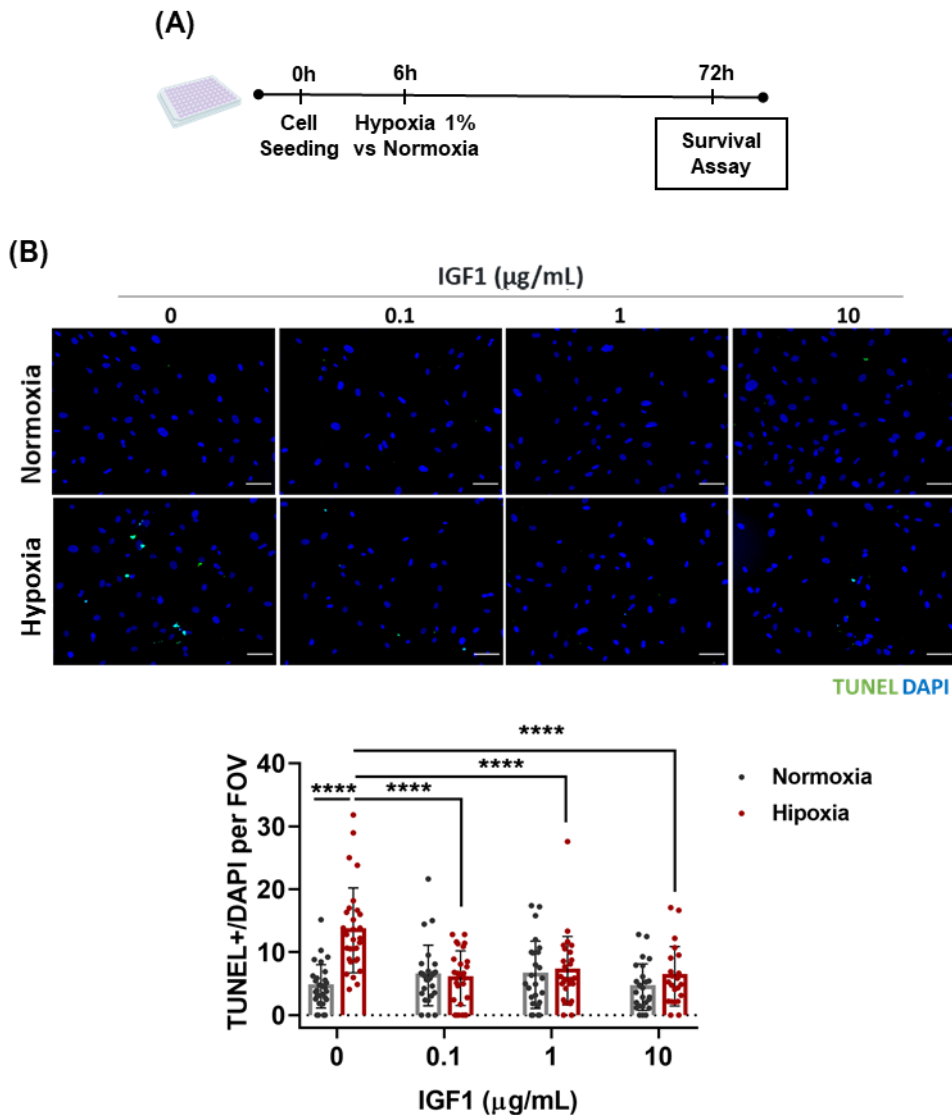


Figure 7 – IGF1 has a protective effect against hypoxia-induced apoptosis in human CFs. (A) Schematic representation of the survival assay using HCFs. (B) Survival evaluation of HCFs subjected to hypoxic conditions (Hypoxia, 1% O₂ for 72h) in the presence or absence of IGF1 (0.1, 1, and 10 $\mu\text{g/mL}$). Cells maintained under normoxic conditions (Normoxia) were used as controls. Upper panel, representative images of the terminal deoxynucleotidyl transferase dUTP nick end labeling (TUNEL) (green) and nuclei staining with DAPI (blue). Scale bar = 100 μm . Lower panel, quantification of TUNEL positive (+) /DAPI counterstained cells at least 700 were counted per condition using Fiji software. The total amount of cells was achieved by counting cell nuclei. TUNEL positive cells were counted manually and divided by the total amount of cells. Statistical significance was tested by One-way ANOVA, and p values for individual comparisons were calculated by Tukey's test. Values are mean \pm SD, $n=1$ **** $p<0.0001$.

Discussion

Ever since antiquity, humanity has questioned, studied, and postulated on the heart's function. Nevertheless, as of this thesis writing, coronary heart disease remains the leading cause of morbidity and death globally¹. Millions of citizens (and their families) struggle with the dependence, wealth, and medical burden caused by MI and heart failure. Newer ways and means of therapy are needed. This work aimed to further our understanding of heart regeneration and repair, emphasizing the role of IGF1 on cardiac fibroblasts, a master regulator of the injury response.

In this thesis, the transcriptome of whole mice hearts during the transition between regenerative and repair window was evaluated by RNAseq to understand the mechanisms involved in the loss of cardiac regenerative capacity after birth. Analysis of differently expressed genes highlighted multiple ECM-associated genes altered between embryonic day E16 and P7, showcasing the important role that the ECM has in the transition between regenerative and reparative periods. These results corroborate other authors' discoveries, such as Ángel Raya's group work demonstrating that ECM stiffness limits cardiac regeneration in neonatal mice⁸⁸ and Bassat et al.'s work demonstrating that agrin (an ECM molecule) is capable of inducing cardiac regeneration post-MI⁹¹.

Of note, in our RNAseq results, multiple IGF family-associated genes were changed, out of which IGF1 was identified as a molecule of interest because of its known role in cell growth and differentiation¹²⁰ and its upregulation in the transition from regenerative to reparative periods. Importantly, IGF1 is a pleiotropic molecule previously associated with cardiomyocytes' growth and proliferation and the matricellular surroundings¹⁴¹.

The RNAseq also identified *Igf2* to be downregulated during the same period, consistent with the previous reports reviewed in¹⁰⁹. However, given that IGF2 is known to be a potent mitogen in the fetal period¹⁰⁹ and has been reported to be involved in cardiac regeneration in neonatal mice¹⁴⁷ exerting most of its function through IGF1R (its other function in nutrient sensing being associated with the insulin receptor¹⁴⁸), it begs the question why would *Igf2* be downregulated and why would a downregulation of *Igf2* be accompanied by an upregulation of *Igf1*, especially considering that both act mainly through IGF1R signaling¹²⁰. One can hypothesize that a potent mitogen such as IGF2 is endogenously downregulated because of the very notion of why cardiac regeneration in humans was not selected in the first place. Namely, because from an evolutionary perspective, MI was not a major relative disadvantage since by the onset of MI, most organisms were already past their fertile period¹⁴⁹, plus the diet of ancient humans did not lend itself to the cardiovascular diseases observed currently¹⁵⁰.

As to why would a downregulation of *Igf2* be concurrent with an *Igf1* upregulation, although there is no definitive answer, it could be argued that since IGF2 can function pleiotropically through the insulin receptor and its downstream pathways and due to the changes in nutrition intake after the birth of the animal, it may be beneficial to have a finer tuning over insulin signaling, hence leading to a downregulation of *Igf2*. IGF1 could perform the mitogenic effect performed by IGF2 (even though IGF2 is not associated with hyperplasia, its hypertrophic capabilities could serve as a functional substitute¹²⁰) hence justifying the *Igf1* upregulation. Effectively, this could mean that growth and nutrient sensing are being, at least partially, regulated by the same signaling mechanisms during the fetal period. However, there would be a split between nutrient sensing and mitogenic pathways after birth, leading to more control over these two essential biological functions. This hypothesis would be concurrent with the prevailing literature since it is known that with the birth of the animal, insulin receptor isoforms switch from IR-A (associated with mitogenic effects)^{148,151} to IR-B (associated with nutrient sensing)¹⁵². Both IGF1 and IGF2 proteins have roughly 5-fold lower affinity to IR-B when compared to IR-A¹⁵³, plus IGF1 has a 10-fold lower affinity to both IRs than IGF2¹⁵³. Together with our results, the hypothesis of splitting signaling pathways with the animal's birth is reinforced.

Following the observed upregulation of *Igf1* in the transitional period between regeneration and repair, we decided to assess IGF family-associated genes expression in the heart in response to MI at P1 (regenerative outcome) and adult animals (reparative response), using a mouse model. In the case of the adult model, a clear upregulation of *Igf1*, *Igfbp3*, *Igfbp4*, *Igfbp7* were observed in the MI region 96h after injury when compared with sham-operated animals. At the same time, no statistically significant difference was found for *Igf2*, *Igfbp5*, *Igfbp6*, and *Htra1*.

A similar experiment in neonatal mice was performed. After injury at P1, the *Igf1* expression contrarily to what was observed in the adult was decreased in the MI group compared with the sham-operated animals at day 3 post-infarction, with the values equaling at day 7 post-infarction. As for *Igf2*, adding to the already existing descending pattern expression after birth, in all neonatal samples observed, the expression of *Igf2* was lower in MI than in sham samples while in the adult model no difference was detected.

The difference in *Igf1* expression between the neonatal and the adult model suggests that IGF1 regulation depends on whether it is in the regenerative or reparative period, implying that *Igf1* function may need to be downregulated for regeneration to occur.

Several questions arise from the adult results: What could be the reasons for *Igf1* upregulation after MI? What are the roles of *Igfbp 3, 4, and 7* in the injury response? Moreover, why does this occur at 96h post-injury?

The latter question, related to the timing where we see these genes' increased expression, could be explained by the complex and multi-phase cardiac repair program⁴⁴. As for the biological reason for *Igf1* upregulation, our results suggest that IGF1 has a role in response to cardiac injury. Whether this role is pro-regenerative or pro-reparative is unclear. Our results and the mouse model used (adult and hence reparative) suggest a reparative role for IGF1 however, this is inconsistent with the scientific literature, which has reported a regenerative and cardioprotective role for IGF1, namely by exerting an antiapoptotic effect on cardiac cells promoting cardiomyocyte proliferation and attenuating angiotensin II-induced cardiac fibrosis^{130,134,141}. However, regarding cardiomyocyte proliferation, it must be taken into account that significant published literature concerning IGF1 and IGF2 considers the number of nuclei as a direct measurement of the number of cardiomyocytes, which is not necessarily correct since binucleation in cardiomyocytes may arrive through hypertrophic and not hyperplastic growth¹⁵⁴.

Simultaneously, it was also observed that *Igf1bp 3, 4, and 7* were upregulated. These IGF-binding proteins have the ability to modulate IGF1 signaling by directly binding IGF1 and prolonging its half-life or by interfering with the IGF1 receptor interaction¹⁰⁷. These molecular mechanisms of IGF family-associated genes lead to a thorough fine-tuning of IGF1 signaling¹⁰⁷. IGFBP3 is the most common of all IGFBPs and has been associated with the stabilization of IGF1 protein¹⁵⁵. As for IGFBP4 and IGFBP7, the former has been known to interfere with IGF1 and IGF1R interaction, hence having a negative impact on its signaling¹⁰⁷. The latter binds weakly to IGF1 and has been reported as a biomarker for MI¹⁵⁶, which our results corroborate. Both the regulation and the very existence of IGFBPs and their correspondent degrading enzymes reinforce the importance of IGF1 signaling because from an evolutionary point of view, only an important pathway would receive such in-depth modulation.

Besides the expression of IGF1, we also looked for the presence of IGF1R on the tissues collected from the adult mice hearts subjected to MI, and an interesting result emerged. IGF1R levels were lower after MI in the infarcted zone compared with the remote zone of the heart and corresponding areas of the heart in sham operated animals. So even though *Igf1* itself is upregulated, its receptor decreases in the same region. This result can be justified by a delay between the expression of the *Igf1r* gene and the production of the protein itself or, the internalization and degradation of the IGF1R could be involved since it has been shown to be a key in the modulation of IGF1 signaling^{97,116}. Another valid hypothesis is that the cells most affected by the MI injury (i.e., cell death) were the ones with higher levels of IGF1R, resulting in an overall lower receptor level. Lastly, it could also be argued that since IGF1 is a secreted molecule, its effects may be not only on the immediate surrounding cells but on more remote areas of the heart.

Based on our results, IGF1 appears to be an essential factor in cardiac remodeling, and its intricate regulation is a part of a multi-phase cardiac repair program, with CFs being responsible for most of its synthesis and secretion, and themselves and cardiomyocytes as targets¹⁴¹. However, an unorthodox argument could be made, namely, that *Igf1* increased expression does not result from the resident heart cells but from immune cells that are recruited and migrate to the heart after injury since it is established that immune cells are necessary for cardiac remodeling¹⁵⁷. This would be consistent with the reported action of macrophages capable of secreting IGF1 (linked to regeneration) in the skeletal muscle¹²⁹. It would also justify why, in the MI models, *Igf1* shows upregulated only after a few days after MI, corresponding to the infiltration and action of the immune cells¹⁵⁸. It is unclear whether immune infiltrate plays a part in the transition from the regenerative and repair period in neonatal mice.

To explore these results' translational potential, we assessed the IGF1 concentration in the pericardial fluid, which is known to concentrate secreted molecules from the heart¹⁵⁹, and plasma of control and with a recent MI and compared them to a control group. Despite the issues regarding this quantification (raised in the results section), a higher concentration of IGF1 was found in the pericardial fluid of our patients after MI, further strengthening that IGF1 is secreted by heart cells during the repair process.

Owing to the opposing regulation of IGF1 during the repair response of the adult and the regenerative response of the neonate, one can speculate that this molecule may be involved in the pro-fibrotic signaling observed in the adult. In line with this, the suppression of *Igf1* expression observed after neonatal injury could be related to the activation of an anti-fibrotic program during regeneration. In fact, our *in vitro* experiments demonstrated that not only *Igf1* is up-regulated upon CF activation, but most importantly, IGF1 per se is able to i) induce mild CF activation and transdifferentiation into myofibroblasts and ii) robustly protect CF for ischemia-induced apoptosis. Despite these effects, no apparent dose-dependent was observed, relating to IGF1 receptor saturation or a downstream pathway reaching a rate-limiting step. Regardless, the results are in line with others that evaluated the effect of IGF1 in CF^{135–137,141}.

The role of CFs in the complex transition from a regenerative to a reparative period remains unclear²⁶. However, they are critical regulators of the injury response¹⁶⁰ and are the main synthesizers of IGF1 in the heart¹⁴¹. To explore the potential effect of IGF1 on cardiac fibroblast we used, an *in vitro* cardiac fibroblast activation model using TGF- β 1 as a mediator of fibroblast differentiation into myofibroblasts in both mouse and human cardiac fibroblast. With this model, we assessed both the *Igf1* expression in activated and non-activated CFs and the effect of exogenous IGF1 in fibroblast activation.

We observed that in both mouse and human CFs, activation by treatment with TGF- β 1 leads to an *Igf1* upregulation, sustained with time. It was also found that human CFs after the same treatment led to a modest increase in the presence of IGF1R. This result corroborates with the autocrine role described for IGF1¹⁶¹.

IGF1 has been reported to be involved in myofibroblast differentiation in the lung, in both *in vivo* (by blocking IGF1R with an antibody) and *in vitro* (by adding IGF1 to cultured cells) model¹³⁵ however, a recent study by Ock et al. using mice models of cardiac fibrosis, demonstrated through both IGF1R knockout and IGF1 infusion that IGF1 is capable of reducing angiotensin-II induced cardiac fibrosis¹⁴⁰. Therefore, our next question was if IGF1 itself could lead to CF activation. We found that when treated with growing concentrations of IGF1, a small but persistent upregulation of activation markers was present, namely α -SMA, Collagen I and CTGF¹⁶². Interestingly this increase in expression of activation markers was not dose-dependent (this will be addressed afterward). We decided to look at the accumulation of α -SMA, the canonical marker for CF activation¹⁶² at a later day of the protocol by immunofluorescence. And found that when treated with IGF1, there was an increase in the number of CFs positive for α -SMA corresponding to CF differentiated into myofibroblasts. However, this increase was not as substantial as when treated with TGF- β 1. The combination TGF- β 1 and IGF1 was not synergetic, despite crosstalk between these two effectors being predicted in the literature^{119,121,163} with Daian et al.¹³⁹ reporting on a synergistic effect between IGF1 and TGF- β 1 regarding the stimulation of ECM production by keloid fibroblasts. Speculating on the reason for the nonexistence of synergy, it could be argued that since there is no noticeable difference between the condition with TGF- β 1 and the condition with both TGF- β 1 and IGF1, the activating pathways responsible may be being subjected to a rate-limiting step. These results indicate that not only IGF-1 is upregulated after CF activation but also is capable of CF activation itself.

Regarding the protective effect of IGF1 on CF, although not previously evaluated in the context of the heart, this protective effect has been shown to be important in other contexts¹⁶⁴ such as vascular endothelial cells reviewed in Conti et al. where IGF is indicated to contribute to the orderly coronary blood flow and stifle endothelial dysfunction through its antiapoptotic effects¹⁶⁵. Plus, IGF1R knockout impaired endothelial function and increased renal fibrosis, leading to kidney disease and dysfunction¹⁶⁶. A similar protective role for IGF1 has been described in neurons after ischemic injury¹⁶⁷. In our experiment, we observed that IGF1 was able to protect human CF from hypoxia - induced apoptosis.

When paired with the upregulation of *Igf1* post-MI in the adult mouse model, these results reinforce the potential protective role of IGF1 after ischemic injury, and therefore depict IGF1 as an essential molecule in the response against MI and the cardiac remodeling thereafter.

In conclusion, we established that IGF1 is a molecule of significant importance in response to ischemic cardiac injury. Our results suggest a reparative role for IGF1 rather than a regenerative one, unlike the prevailing literature. This may have implications for future studies and the development (or not) of newer therapies regarding restoration of healthy tissue function. How could this be justified? Our *in vivo* results do not necessarily dismiss a regenerative role but simply associate endogenous *Igf1* expression with a known reparative period rather than a regenerative one. As for our cell culture results, again, these do not disprove a regenerative role but simply describe that IGF1 has previously undescribed roles in cardiac fibroblasts and that it may help the latter accomplish its function in cardiac remodeling, in either repair or regeneration. This would be consistent with a previous model of neonatal regeneration described by the group in which a hybrid model is proposed⁸⁴ where after injury, both regenerative and repair mechanisms seem to be active⁸⁴.

Conclusion and future perspectives

Understanding the molecular mechanisms and key players that mediate the cardiac response to injury represents an effective tool for discovering new therapeutic targets that may integrate anti-fibrotic therapies. Herein, we provide new insights into the potential role of IGF1, an autocrine and paracrine signaling molecule produced by cardiac fibroblasts in response to ischemic injury in the heart.

The primary findings of our research are that IGF1 is differentially regulated after ischemic injury between the neonatal (regenerative response) and adult (reparative response) timepoints, with IGF1 being upregulated after MI in the adult mouse model. Plus, we found that IGF1 can induce cardiac fibroblast activation and promote cardiac fibroblast survival in a hypoxic setting correlating with a reparative response upon injury.

Altogether, our budding results suggest that IGF1 is involved in the transition from the regenerative to reparative response through the mechanism of fibroblast activation and that IGF1 action may be suppressed in the post-natal period. Therefore, our future experiments should:

- Include an *in vivo* assay on neonatal mice treated with IGF1 to investigate if IGF1 can induce an early reparative response (ongoing).
- Determine if IGF1 has any role in the establishment of binucleation in cardiomyocytes.
- Evaluate if IGF1 can rescue cardiomyocytes from hypoxia-induced cell death.

Therefore, these studies should i) Establish a solid foundation for the role of IGF1 and cardiac fibroblast in the heart ii) Further our understanding of IGF1 in both neonatal and adult cardiomyocytes.

We anticipate with expectation that our contributions may lead our community to a greater understanding of itself and the pathologies studied, ultimately shepherding a better clinical outcome for patients.

References

1. Virani, S. S. *et al.* Heart disease and stroke statistics—2020 update: A report from the American Heart Association. *Circulation* vol. 141 E139–E596 (2020).
2. Libby, P. *et al.* Atherosclerosis. *Nat. Rev. Dis. Prim.* **5**, 1–18 (2019).
3. Kong, P. *et al.* The pathogenesis of cardiac fibrosis. *Cellular and Molecular Life Sciences* vol. 71 549–574 (2014).
4. Weinhaus, A. J. & Roberts, K. P. Anatomy of the Human Heart. *Handb. Card. Anatomy, Physiol. Devices* 51–79 (2005)
5. Rodriguez, E. R. & Tan, C. D. Structure and Anatomy of the Human Pericardium. *Prog. Cardiovasc. Dis.* **59**, 327–340 (2017).
6. Goldsmith, E. C. *et al.* Organization of fibroblasts in the heart. *Dev. Dyn.* **230**, 787–794 (2004).
7. Yue, B. Biology of the extracellular matrix: An overview. *Journal of Glaucoma* vol. 23 S20–S23 (2014).
8. Skandalis, S. *et al.* Impact of Extracellular Matrix on Cellular Behavior: A Source of Molecular Targets in Disease. *BioMed Research International* vol. 2015 (2015).
9. Silva, A. C. *et al.* Three-dimensional scaffolds of fetal decellularized hearts exhibit enhanced potential to support cardiac cells in comparison to the adult. *Biomaterials* **104**, 52–64 (2016).
10. Hanson, K. P. *et al.* Spatial and Temporal Analysis of Extracellular Matrix Proteins in the Developing Murine Heart: A Blueprint for Regeneration. *Tissue Eng. Part A* **19**, 1132 (2013).
11. Bedore, J. *et al.* Targeting the extracellular matrix: Matricellular proteins regulate cell-extracellular matrix communication within distinct niches of the intervertebral disc. *Matrix Biology* vol. 37 124–130 (2014).
12. Bornstein, P. Matricellular proteins: An overview. *Journal of Cell Communication and Signaling* vol. 3 163–165 (2009).
13. Schellings, M. *et al.* Matricellular proteins in the heart: Possible role during stress and remodeling. *Cardiovascular Research* vol. 64 24–31 (2004).

14. Bedore, J. *et al.* Targeting the extracellular matrix: Matricellular proteins regulate cell-extracellular matrix communication within distinct niches of the intervertebral disc. *Matrix Biology* vol. 37 124–130 (2014).
15. Wong, G. S. & Rustgi, A. K. Matricellular proteins: Priming the tumour microenvironment for cancer development and metastasis. *British Journal of Cancer* vol. 108 755–761 (2013).
16. Khokha, R. *et al.* Metalloproteinases and their natural inhibitors in inflammation and immunity. *Nature Reviews Immunology* vol. 13 649–665 (2013).
17. Morris, A. H. & Kyriakides, T. R. Matricellular proteins and biomaterials. *Matrix Biology* vol. 37 183–191 (2014).
18. Jun, J. II & Lau, L. F. Taking aim at the extracellular matrix: CCN proteins as emerging therapeutic targets. *Nature Reviews Drug Discovery* vol. 10 945–963 (2011).
19. Lockhart, M. *et al.* Extracellular matrix and heart development. *Birth Defects Res. A. Clin. Mol. Teratol.* **91**, 535–550 (2011).
20. Willian P, D. *et al.* Extracellular matrix dynamics in development and regenerative medicine. *J. Cell Sci.* **121**, 255–264 (2008).
21. Ivey, M. J. & Tallquist, M. D. Defining the Cardiac Fibroblast: A New Hope. *Circ. J.* **80**, 2269 (2016).
22. Snider, P. *et al.* Origin of cardiac fibroblasts and the role of periostin. *Circ. Res.* **105**, 934–947 (2009).
23. Vasquez, C. *et al.* The Cardiac Fibroblast: Functional and Electrophysiological Considerations in Healthy and Diseased Hearts. *J. Cardiovasc. Pharmacol.* **57**, 380 (2011).
24. Hodgkinson, C. P. *et al.* Emerging Concepts in Paracrine Mechanisms in Regenerative Cardiovascular Medicine and Biology. *Circ. Res.* **118**, 95 (2016).
25. Tallquist, M. D. Cardiac fibroblasts: from origin to injury. *Current Opinion in Physiology* vol. 1 75–79 (2018).
26. Tallquist, M. D. & Molkenin, J. D. Redefining the identity of cardiac fibroblasts. *Nature Reviews Cardiology* vol. 14 484–491 (2017).

27. Kanisicak, O. *et al.* Genetic lineage tracing defines myofibroblast origin and function in the injured heart. *Nat. Commun.* **7**, 1–14 (2016).
28. Acharya, A. *et al.* The bHLH transcription factor Tcf21 is required for lineagespecific EMT of cardiac fibroblast progenitors. *Dev.* **139**, 2139–2149 (2012).
29. Acharya, A., *et al.* Efficient inducible Cre-mediated recombination in Tcf21 cell lineages in the heart and kidney. *Genesis* **49**, 870–877 (2011).
30. Braitsch, C. M. *et al.* Pod1/Tcf21 is regulated by retinoic acid signaling and inhibits differentiation of epicardium-derived cells into smooth muscle in the developing heart. *Dev. Biol.* **368**, 345–357 (2012).
31. Pinto, A. R. *et al.* Revisiting cardiac cellular composition. *Circ. Res.* **118**, 400–409 (2016).
32. Van Berlo, J. H. & Molkentin, J. D. An emerging consensus on cardiac regeneration. *Nature Medicine* vol. 20 1386–1393 (2014).
33. Frangogiannis, N. G. The inflammatory response in myocardial injury, repair, and remodelling. *Nature Reviews Cardiology* vol. 11 255–265 (2014).
34. Hall, C., *et al.* Complex Relationship Between Cardiac Fibroblasts and Cardiomyocytes in Health and Disease. *J. Am. Heart Assoc.* **10**, 1–15 (2021).
35. Zhang, Y. E. Non-Smad pathways in TGF- β signaling. *Cell Res.* 2009 191 **19**, 128–139 (2008).
36. Huang, Y. *et al.* MicroRNA-21: a central regulator of fibrotic diseases via various targets. *Curr. Pharm. Des.* **21**, 2236–2242 (2015).
37. Meng, X., *et al.* TGF- β : the master regulator of fibrosis. *Nat. Rev. Nephrol.* 2016 126 **12**, 325–338 (2016).
38. Elliot, S. *et al.* MicroRNA let-7 Downregulates Ligand-Independent Estrogen Receptor-mediated Male-Predominant Pulmonary Fibrosis. *Am. J. Respir. Crit. Care Med.* **200**, 1246–1257 (2019).
39. Rockey, D. C. *et al.* Smooth Muscle α Actin (Acta2) and Myofibroblast Function during Hepatic Wound Healing. *PLoS One* **8**, e77166 (2013).
40. Hinz, B. Myofibroblasts. *Exp. Eye Res.* **142**, 56–70 (2016).

41. Stempien-Otero, A., *et al.* Molecular networks underlying myofibroblast fate and fibrosis. *Journal of Molecular and Cellular Cardiology* vol. 97 153–161 (2016).
42. Bergmann, O. *et al.* Evidence for cardiomyocyte renewal in humans. *Science (80-.)*. **324**, 98–102 (2009).
43. Ziaeeian, B. & Fonarow, G. C. Epidemiology and aetiology of heart failure. *Nature Reviews Cardiology* vol. 13 368–378 (2016).
44. Prabhu, S. D. & Frangogiannis, N. G. The biological basis for cardiac repair after myocardial infarction. *Circulation Research* vol. 119 91–112 (2016).
45. Eltzschig, H. K. & Eckle, T. Ischemia and reperfusion—from mechanism to translation. *Nature Medicine* vol. 17 1391–1401 (2011).
46. De Haan, J. *et al.* Danger signals in the initiation of the inflammatory response after myocardial infarction. *Mediators of Inflammation* vol. 2013 (2013).
47. Lin, L. & Knowlton, A. A. Innate immunity and cardiomyocytes in ischemic heart disease. *Life Sciences* vol. 100 1–8 (2014).
48. Ghigo, A., *et al.* Myocyte signalling in leucocyte recruitment to the heart. *Cardiovascular Research* vol. 102 270–280 (2014).
49. Zhang, W. *et al.* Necrotic myocardial cells release Damage-Associated Molecular Patterns that provoke fibroblast activation in vitro and trigger myocardial inflammation and fibrosis in vivo. *J. Am. Heart Assoc.* **4**, (2015).
50. Casanova, J. *et al.* Human TLRs and IL-1Rs in Host Defense: Natural Insights from Evolutionary, Epidemiological, and Clinical Genetics. *Annu. Rev. Immunol.* **29**, 447–491 (2011).
51. Mann, D. L. The emerging role of innate immunity in the heart and vascular system: For whom the cell tolls. *Circ. Res.* **108**, 1133–1145 (2011).
52. Newton, K. & Dixit, V. M. Signaling in innate immunity and inflammation. *Cold Spring Harb. Perspect. Biol.* **4**, (2012).
53. Schroder, K. & Tschopp, J. The Inflammasomes. *Cell* vol. 140 821–832 (2010).

54. Nian, M. *et al.* Inflammatory cytokines and postmyocardial infarction remodeling. *Circulation Research* vol. 94 1543–1553 (2004).
55. Frangogiannis, N. G. The extracellular matrix in myocardial injury, repair, and remodeling. *J. Clin. Invest.* **127**, 1600 (2017).
56. Zeisberg, E. M. & Kalluri, R. Origins of cardiac fibroblasts. *Circ. Res.* **107**, 1304–1312 (2010).
57. Wei, S. *et al.* Left and right ventricular collagen type I/III ratios and remodeling post-myocardial infarction. *J. Card. Fail.* **5**, 117–126 (1999).
58. McCurdy, S. *et al.* Cardiac extracellular matrix remodeling: Fibrillar collagens and secreted protein Acidic and Rich in Cysteine (SPARC). *Journal of Molecular and Cellular Cardiology* vol. 48 544–549 (2010).
59. Silva, A. C. *et al.* Bearing My Heart: The Role of Extracellular Matrix on Cardiac Development, Homeostasis, and Injury Response. *Front. Cell Dev. Biol.* **8**, (2020).
60. Broughton, K. M. *et al.* Mechanisms of Cardiac Repair and Regeneration. *Circ. Res.* **122**, 1151–1163 (2018).
61. González, A. *et al.* The complex dynamics of myocardial interstitial fibrosis in heart failure. Focus on collagen cross-linking. *Biochimica et Biophysica Acta - Molecular Cell Research* vol. 1866 1421–1432 (2019).
62. Soehnlein, O. & Lindbom, L. Phagocyte partnership during the onset and resolution of inflammation. *Nature Reviews Immunology* vol. 10 427–439 (2010).
63. De Mello, W. C. & Danser, A. H. J. Angiotensin II and the heart on the intracrine renin-angiotensin system. *Hypertension* vol. 35 1183–1188 (2000).
64. Frangogiannis, N. G. Transforming growth factor- β in tissue fibrosis. *Journal of Experimental Medicine* vol. 217 (2020).
65. Christia, P. *et al.* Systematic Characterization of Myocardial Inflammation, Repair, and Remodeling in a Mouse Model of Reperfused Myocardial Infarction. *J. Histochem. Cytochem.* **61**, 555–570 (2013).
66. Frangogiannis, N. G. *et al.* Myofibroblasts in reperfused myocardial infarcts express the embryonic form of smooth muscle myosin heavy chain (SMemb). *Cardiovasc. Res.* **48**, 89–100

(2000).

67. Echeverri, K. & Zayas, R. M. Regeneration: From cells to tissues to organisms. *Developmental Biology* vol. 433 109–110 (2018).
68. Jopling, C. *et al.* Dedifferentiation, transdifferentiation and reprogramming: Three routes to regeneration. *Nature Reviews Molecular Cell Biology* vol. 12 79–89 (2011).
69. Zakrzewski, W. *et al.* Stem cells: Past, present, and future. *Stem Cell Research and Therapy* vol. 10 68 (2019).
70. Cai, S., Fu, X. & Sheng, Z. Dedifferentiation: A New Approach in Stem Cell Research. *Bioscience* **57**, 655–662 (2007).
71. Yao, Y. & Wang, C. Dedifferentiation: inspiration for devising engineering strategies for regenerative medicine. *npj Regenerative Medicine* vol. 5 1–11 (2020).
72. Porrello, E. R. *et al.* Transient regenerative potential of the neonatal mouse heart. *Science (80-.)*. **331**, 1078–1080 (2011).
73. Ahuja, P., Sdek, P. & MacLellan, W. R. Cardiac myocyte cell cycle control in development, disease, and regeneration. *Physiological Reviews* vol. 87 521–544 (2007).
74. Derks, W. & Bergmann, O. Polyploidy in Cardiomyocytes. *Circ. Res.* 552–565 (2020)
75. Puente, B. N. *et al.* The Oxygen Rich Postnatal Environment Induces Cardiomyocyte Cell Cycle Arrest Through DNA Damage Response. *Cell* **157**, 565 (2014).
76. Nakada, Y. *et al.* Hypoxia induces heart regeneration in adult mice. *Nat. Publ. Gr.* (2017)
77. Chattergoon, N. Thyroid Hormone Signalling and consequences for cardiac development. *J. Endocrinol.* **242**, T145 (2019).
78. Nakada, Y. *et al.* DNA Damage Response Mediates Pressure Overload–Induced Cardiomyocyte Hypertrophy. *Circulation* **139**, 1237–1239 (2019).
79. Gan, P. *et al.* Cardiomyocyte Polyploidy and Implications for Heart Regeneration. *82*, 45–61 (2020).
80. Ausoni, S. & Sartore, S. From fish to amphibians to mammals: In search of novel strategies to

optimize cardiac regeneration. *Journal of Cell Biology* vol. 184 357–364 (2009).

81. Laube, F. *et al.* Re-programming of newt cardiomyocytes is induced by tissue regeneration. *J. Cell Sci.* **119**, 4719–4729 (2006).
82. Stockdale, W. T. *et al.* Heart Regeneration in the Mexican Cavefish. *Cell Rep.* **25**, 1997-2007.e7 (2018).
83. Major, R. J. *et al.* Zebrafish heart regeneration as a model for cardiac tissue repair. *Drug Discovery Today: Disease Models* vol. 4 219–225 (2007).
84. Sampaio-Pinto, V. *et al.* Neonatal Apex Resection Triggers Cardiomyocyte Proliferation, Neovascularization and Functional Recovery Despite Local Fibrosis. *Stem Cell Reports* **10**, 860–874 (2018).
85. Polizzotti, B. D. *et al.* A cryoinjury model in neonatal mice for cardiac translational and regeneration research. *Nat. Protoc.* **11**, 542–552 (2016).
86. Haubner, B. J. *et al.* Complete cardiac regeneration in a mouse model of myocardial infarction. *Aging (Albany, NY).* **4**, 966–977 (2012).
87. Haubner, B. J. *et al.* A reproducible protocol for neonatal ischemic injury and cardiac regeneration in neonatal mice. *Basic Res. Cardiol.* **111**, (2016).
88. Notari, M. *et al.* The local microenvironment limits the regenerative potential of the mouse neonatal heart. *Sci. Adv.* **4**, eaao5553 (2018).
89. Silva, A. C. *et al.* Three-dimensional scaffolds of fetal decellularized hearts exhibit enhanced potential to support cardiac cells in comparison to the adult. *Biomaterials* **104**, 52–64 (2016).
90. Kühn, B. *et al.* Periostin induces proliferation of differentiated cardiomyocytes and promotes cardiac repair. *Nat. Med.* **2007 138 13**, 962–969 (2007).
91. Bassat, E. *et al.* The extracellular matrix protein agrin promotes heart regeneration in mice. *Nat.* **2017 5477662 547**, 179–184 (2017).
92. Wang, Y. *et al.* Single-cell analysis of murine fibroblasts identifies neonatal to adult switching that regulates cardiomyocyte maturation. *Nat. Commun.* **2020 111 11**, 1–18 (2020).
93. Sadek, H. & Olson, E. N. Cell Stem Cell Review Toward the Goal of Human Heart

Regeneration. *Stem Cell* **26**, 7–16 (2020).

94. Rho, O. *et al.* Growth factor signaling pathways as targets for prevention of epithelial carcinogenesis. *Mol. Carcinog.* **50**, 264–279 (2011).
95. Laron, Z. Insulin-like growth factor 1 (IGF-1): A growth hormone. *J. Clin. Pathol. - Mol. Pathol.* **54**, 311–316 (2001).
96. Kavran, J. M. *et al.* How IGF-1 activates its receptor. *Elife* **3**, (2014).
97. Faveyukis, S. *et al.* Structure and autoregulation of the insulin-like growth factor 1 receptor kinase. *Nat. Struct. Biol.* **8**, 1058–1063 (2001).
98. Blum, W. F. *et al.* The growth hormone-insulin-like growth factor-I axis in the diagnosis and treatment of growth disorders. *Endocrine Connections* vol. 7 R212–R222 (2018).
99. Oberbauer, A. M. The Regulation of IGF-1 Gene Transcription and Splicing during Development and Aging. *Front. Endocrinol. (Lausanne)*. **4**, (2013).
100. Gilmour, R. S. The implications of insulin-like growth factor mRNA heterogeneity. *J. Endocrinol.* **140**, 1–3 (1994).
101. O'Sullivan, D. C. *et al.* Regulation of hepatic insulin-like growth factor I leader exon usage in lambs: Effect of immunization against growth hormone-releasing factor and subsequent growth hormone treatment. *J. Anim. Sci.* **80**, 1074–1082 (2002).
102. Ohlsson, C. *et al.* The role of liver-derived insulin-like growth factor-I. *Endocrine Reviews* vol. 30 494–535 (2009).
103. Wang, Y. *et al.* Autocrine and Paracrine Actions of IGF-I Signaling in Skeletal Development. *Bone Research* vol. 1 249–259 (2013).
104. Takeshi, H. *et al.* Production and autocrine/paracrine effects of endogenous insulin-like growth factor-1 in rat cardiac fibroblasts. *Regul. Pept.* **124**, 65–72 (2005).
105. Hu, S. I. *et al.* Human HtrA, an evolutionarily conserved serine protease identified as a differentially expressed gene product in osteoarthritic cartilage. *J. Biol. Chem.* **273**, 34406–34412 (1998).
106. Cohick, W. S. & Clemmons, D. R. The insulin-like growth factors. *Annual Review of Physiology*

vol. 55 131–153 (1993).

107. Allard, J. B. & Duan, C. IGF-binding proteins: Why do they exist and why are there so many? *Frontiers in Endocrinology* vol. 9 1 (2018).
108. Li, Y., Xiang, J. & Duan, C. Insulin-like growth factor-binding protein-3 plays an important role in regulating pharyngeal skeleton and inner ear formation and differentiation. *J. Biol. Chem.* **280**, 3613–3620 (2005).
109. Bergman, D. *et al.* Insulin-Like Growth Factor 2 in Development and Disease: A Mini-Review. *Gerontology* **59**, 240–249 (2013).
110. Engström, W. *et al.* Transcriptional regulation and biological significance of the insulin like growth factor II gene. *Cell Prolif.* **31**, 173–189 (1998).
111. Hellström, A. *et al.* Role of Insulinlike Growth Factor 1 in Fetal Development and in the Early Postnatal Life of Premature Infants. *Am. J. Perinatol.* **33**, 1067–1071 (2016).
112. Löfqvist, C. *et al.* Reference Values for IGF-I throughout Childhood and Adolescence: A Model that Accounts Simultaneously for the Effect of Gender, Age, and Puberty. *J. Clin. Endocrinol. Metab.* **86**, 5870–5876 (2001).
113. Chanson, P. *et al.* Reference Values for IGF-I Serum Concentrations: Comparison of Six Immunoassays. *J. Clin. Endocrinol. Metab.* **101**, 3450 (2016).
114. Li, J. *et al.* chen. Structural basis of the activation of type 1 insulin-like growth factor receptor. *Nat. Commun.* **10**, 1–11 (2019).
115. Shen, H. *et al.* Mononuclear diploid cardiomyocytes support neonatal mouse heart regeneration in response to paracrine IGF2 signaling. *Elife* **9**, (2020).
116. Adams, T. E. *et al.* Structure and function of the type 1 insulin-like growth factor receptor. *Cellular and Molecular Life Sciences* vol. 57 1050–1093 (2000).
117. Girnita, Li. *et al.* Something old, something new and something borrowed: emerging paradigm of insulin-like growth factor type 1 receptor (IGF-1R) signaling regulation. *Cell. Mol. Life Sci.* **71**, 2403 (2014).
118. Crudden, C. *et al.* Below the Surface: IGF-1R Therapeutic Targeting and Its Endocytic Journey. *Cells* **8**, (2019).

119. Manning, B. D. & Toker, A. Leading Edge Review AKT/PKB Signaling: Navigating the Network. *Cell* **169**, 381–405 (2017).
120. Troncoso, R. *et al.* New insights into IGF-1 signaling in the heart. *Trends in Endocrinology and Metabolism* vol. 25 128–137 (2014).
121. McCubrey, J. A. *et al.* Roles of the Raf/MEK/ERK pathway in cell growth, malignant transformation and drug resistance. *Biochimica et Biophysica Acta - Molecular Cell Research* vol. 1773 1263–1284 (2007).
122. Foncea, R. *et al.* Extracellular regulated kinase, but not protein kinase C, is an antiapoptotic signal of insulin-like growth factor-1 on cultured cardiac myocytes. *Biochem. Biophys. Res. Commun.* **273**, 736–744 (2000).
123. Colao, A. The GH-IGF-I axis and the cardiovascular system: clinical implications. *Clin. Endocrinol. (Oxf)*. **69**, 347–358 (2008).
124. Duerr, R. L. *et al.* Insulin-like growth factor-1 enhances ventricular hypertrophy and function during the onset of experimental cardiac failure. *J. Clin. Invest.* **95**, 619 (1995).
125. Rubin, S., Fishbein, M. & Swan, H. Compensatory hypertrophy in the heart after myocardial infarction in the rat. *J. Am. Coll. Cardiol.* **1**, 1435–1441 (1983).
126. Li, Q. *et al.* Overexpression of insulin-like growth factor-1 in mice protects from myocyte death after infarction, attenuating ventricular dilation, wall stress, and cardiac hypertrophy. *J. Clin. Invest.* **100**, 1991–1999 (1997).
127. Santini, M. P. *et al.* Enhancing Repair of the Mammalian Heart. *Circ. Res.* **100**, 1732–1740 (2007).
128. Heinen, A. *et al.* IGF1 Treatment Improves Cardiac Remodeling after Infarction by Targeting Myeloid Cells. *Mol. Ther.* **27**, 46–58 (2019).
129. Tonkin, J. *et al.* Monocyte/Macrophage-derived IGF-1 Orchestrates Murine Skeletal Muscle Regeneration and Modulates Autocrine Polarization. *Mol. Ther.* **23**, 1189–1200 (2015).
130. Báez-Díaz, C. *et al.* Microencapsulated Insulin-Like Growth Factor-1 therapy improves cardiac function and reduces fibrosis in a porcine acute myocardial infarction model. *Sci. Reports* 2020 **10**, 1–11 (2020).

131. O'Sullivan, J. F. *et al.* Potent Long-Term Cardioprotective Effects of Single Low-Dose Insulin-Like Growth Factor-1 Treatment Postmyocardial Infarction. *Circ. Cardiovasc. Interv.* **4**, 327–335 (2011).
132. Crick, S. J. *et al.* Gebstein, L. & Anderson, R. H. Anatomy of the pig heart: comparisons with normal human cardiac structure. *J. Anat.* **193**, 105 (1998).
133. Ceccato, T. L. *et al.* Defining the Cardiac Fibroblast Secretome in a Fibrotic Microenvironment. *J. Am. Heart Assoc.* **9**, 17025 (2020).
134. McDevitt, T. *et al.* Proliferation of cardiomyocytes derived from human embryonic stem cells is mediated via the IGF/PI 3-kinase/Akt signaling pathway. *J. Mol. Cell. Cardiol.* **39**, 865–873 (2005).
135. Hung, C. *et al.* Role of IGF-1 pathway in lung fibroblast activation. *Respir. Res.* **14**, (2013).
136. Reiss, K. *et al.* Fibroblast proliferation during myocardial development in rats is regulated by IGF-1 receptors. *Am. J. Physiol. - Hear. Circ. Physiol.* **269**, (1995).
137. Diaz-Araya, G. *et al.* IGF-1 Modulation of Rat Cardiac Fibroblast Behavior and Gene Expression is Age-Dependent. *Cell Commun. Adhes.* **10**, 155–165 (2003).
138. Li, G. *et al.* Antifibrotic cardioprotection of berberine via downregulating myocardial IGF-1 receptor-regulated MMP-2/MMP-9 expression in diabetic rats. *Am. J. Physiol. - Hear. Circ. Physiol.* **315**, H802–H813 (2018).
139. Daian, T. *et al.* Insulin-Like Growth Factor-I Enhances Transforming Growth Factor- β -Induced Extracellular Matrix Protein Production Through the P38/Activating Transcription Factor-2 Signaling Pathway in Keloid Fibroblasts. *J. Invest. Dermatol.* **120**, 956–962 (2003).
140. Ock, S. *et al.* IGF-1 protects against angiotensin II-induced cardiac fibrosis by targeting α SMA. *Cell Death Dis.* **2021 127 12**, 1–10 (2021).
141. Takeda, N. *et al.* Cardiac fibroblasts are essential for the adaptive response of the murine heart to pressure overload. *J. Clin. Invest.* **120**, 254–265 (2010).
142. Schneider, C. A. *et al.* NIH Image to ImageJ: 25 years of image analysis. *Nature Methods* vol. 9 671–675 (2012).
143. Wang, Z. *et al.* Mechanistic basis of neonatal heart regeneration revealed by transcriptome

- and histone modification profiling. *Proc. Natl. Acad. Sci.* **116**, 18455–18465 (2019).
144. Naba, A. *et al.* Towards definition of an ECM parts list: An advance on GO categories. *Matrix Biol.* **31**, 371 (2012).
 145. Hynes, R. O. & Naba, A. Overview of the Matrisome—An Inventory of Extracellular Matrix Constituents and Functions. *Cold Spring Harb. Perspect. Biol.* **4**, (2012).
 146. Stiles, A. D. & D'Ercole, A. J. The insulin-like growth factors and the lung. *Am. J. Respir. Cell Mol. Biol.* **3**, 93–100 (1990).
 147. Shen, H. *et al.* Mononuclear diploid cardiomyocytes support neonatal mouse heart regeneration in response to paracrine IGF2 signaling. *Elife* **9**, (2020).
 148. Pandini, G. *et al.* IGF-II binding to insulin receptor isoform A induces a partially different gene expression profile from insulin binding. *Ann. N. Y. Acad. Sci.* **1028**, 450–456 (2004).
 149. Ding, K. & Kullo, I. J. Evolutionary Genetics of Coronary Heart Disease. *Circulation* **119**, 459–467 (2009).
 150. O'Keefe, J. H. & Cordain, L. Cardiovascular Disease Resulting From a Diet and Lifestyle at Odds With Our Paleolithic Genome: How to Become a 21st-Century Hunter-Gatherer. *Mayo Clin. Proc.* **79**, 101–108 (2004).
 151. Frasca, F. *et al.* Insulin receptor isoform A, a newly recognized, high-affinity insulin-like growth factor II receptor in fetal and cancer cells. *Mol. Cell. Biol.* **19**, 3278–3288 (1999).
 152. Belfiore, A. *et al.* Insulin Receptor Isoforms in Physiology and Disease: An Updated View. *Endocr. Rev.* **38**, 379–431 (2017).
 153. Andersen, M. *et al.* IGF1 and IGF2 specificities to the two insulin receptor isoforms are determined by insulin receptor amino acid 718. *PLoS One* **12**, (2017).
 154. Derks, W. & Bergmann, O. Polyploidy in Cardiomyocytes. *Circ. Res.* 552–565 (2020).
 155. Hey, A. W. *et al.* Purification and characterization of a fetal somatomedin from the sheep: Similarity to insulin-like growth factor II. *Endocrinology* **122**, 12–21 (1988).
 156. Lisowska, A. *et al.* Insulin-like growth factor-binding protein 7 (IGFBP 7) as a new biomarker in coronary heart disease. *Adv. Med. Sci.* **64**, 195–201 (2019).

157. Frangogiannis, N. G. Regulation of the inflammatory response in cardiac repair. *Circulation Research* vol. 110 159–173 (2012).
158. Lai, S. *et al.* Immune responses in cardiac repair and regeneration: a comparative point of view. *Cell. Mol. Life Sci.* **76**, 1365 (2019).
159. Trindade, F. *et al.* Pericardial fluid: an underrated molecular library of heart conditions and a potential vehicle for cardiac therapy. *Basic Res. Cardiol.* **114**, (2019).
160. Chen, W. & Frangogiannis, N. G. Fibroblasts in post-infarction inflammation and cardiac repair. *Biochimica et Biophysica Acta - Molecular Cell Research* vol. 1833 945–953 (2013).
161. T, H. *et al.* Production and autocrine/paracrine effects of endogenous insulin-like growth factor-1 in rat cardiac fibroblasts. *Regul. Pept.* **124**, 65–72 (2005).
162. Ma, Y. *et al.* Cardiac Fibroblast Activation Post-Myocardial Infarction: Current Knowledge Gaps. *Trends Pharmacol. Sci.* **38**, 448 (2017).
163. Hall, C. *et al.* Complex Relationship Between Cardiac Fibroblasts and Cardiomyocytes in Health and Disease. *J. Am. Heart Assoc.* **10**, 1–15 (2021).
164. Liu, Q. *et al.* Insulin-like growth factor 1 receptor-mediated cell survival in hypoxia depends on the promotion of autophagy via suppression of the PI3K/Akt/mTOR signaling pathway. *Mol. Med. Rep.* **15**, 2136–2142 (2017).
165. Conti, E. *et al.* Insulin-Like Growth Factor-1 as a Vascular Protective Factor. *Circulation* **110**, 2260–2265 (2004).
166. Liang, M. *et al.* Protective Role of Insulin-Like Growth Factor-1 Receptor in Endothelial Cells against Unilateral Ureteral Obstruction–Induced Renal Fibrosis. *Am. J. Pathol.* **185**, 1234 (2015).
167. Liu, W. *et al.* Blunting type 1 insulin-like growth factor receptor expression exacerbates neuronal apoptosis following hypoxic/ischemic injury. *BMC Neurosci.* 2011 121 **12**, 1–11 (2011).

Supplementary Data

Supplementary materials

Quantification of IGF1 in human pericardial fluid and plasma by ELISA

Peripheral blood and pericardial fluid (PF) were collected from two patient cohorts undergoing coronary artery bypass grafting: i) a control, stable coronary artery patients (stable angina, without previous MI or acute coronary syndrome) and ii) a MI group, composed of patients with a recent first MI episode (maximum 3 months before surgery). The two groups were characterized in terms of age, sex, age, cardiovascular risk factors, and medication at the time of surgery. The MI group comprised two types of patients: the STEMI, patients with ST-elevation myocardial infarction, and the NSTEMI, patients with non-ST-elevation myocardial infarction.

Quantification of the free form of IGF1 in PF and plasma samples collected from the MI and control patients was performed using an enzyme-linked immunosorbent assay (ELISA) kit for detecting human IGF1 (RayBiotech #ELH-IGF1-1) according to the manufacturer's instructions. Briefly, biological samples and standards were incubated in sealed wells for 2 h and 30 min. They were washed and added a previously prepared biotinylated antibody solution, and incubated for 1h. Wells were washed and incubated for 45 min with horseradish peroxidase (HRP)-coupled streptavidin solution. Wells were washed once again and incubated with a 3,3',5,5'-tetramethylbenzidine (TMB) solution for 30 min. This step yields a blue color caused by the oxidation of TMB as a result of the hydrolysis of hydrogen peroxide by HRP. To stop the before-mentioned reaction, a solution containing sulfuric acid was added to the wells after incubation, changing the color of the solution to yellow. The absorbance was then read immediately at 450 nm in a Synergy™ Mx Microplate Reader (BioTek). All incubations were done at room temperature and in slight agitation.

Supplementary figures

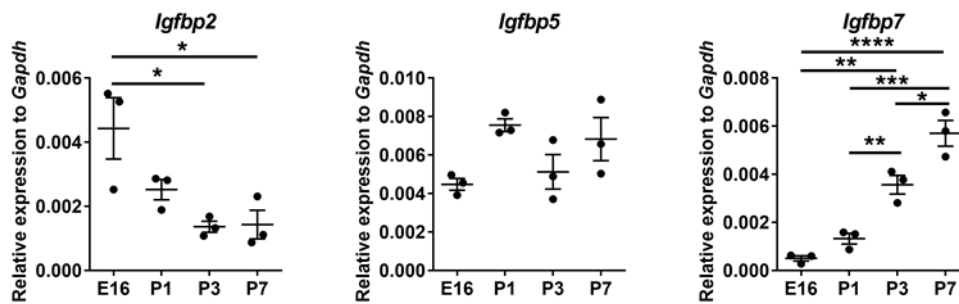


Figure S1 – Validation by qPCR of RNAseq results of *Igfbp2*, *Igfbp5* and *Igfbp7* expression in mouse heart ventricles. Data was normalized to *Gapdh*, statistical significance was tested by One-way ANOVA and p values for individual comparisons were calculated by Tukey's test. values are mean \pm SD, $n=3$, * $p<0.05$; ** $p<0.01$, *** $p<0.001$, **** $p<0.0001$.

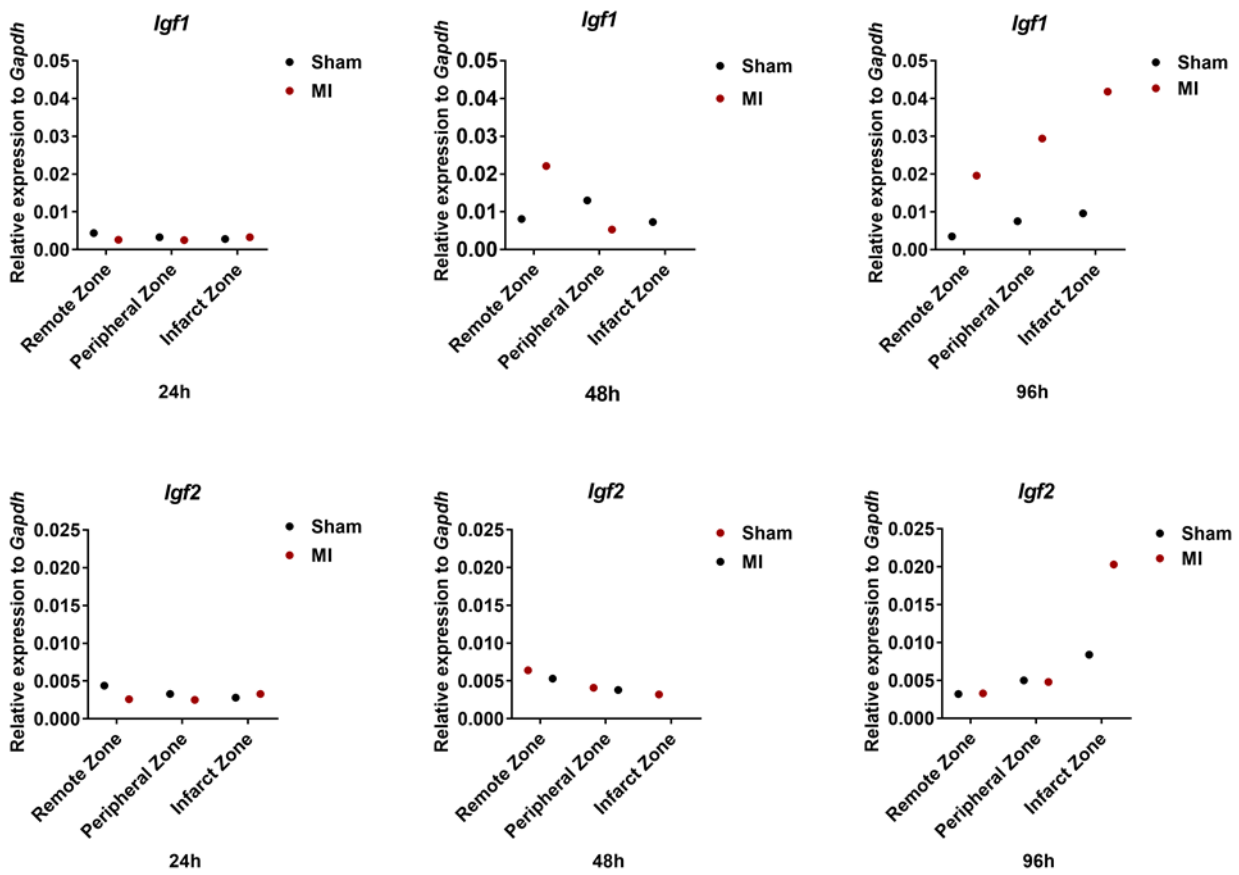


Figure S2 - *Igf1* and *Igf2* expression analyzed by qPCR at different timepoints (24h; 48 and 96h) after injury in an adult mice MI model. Heart tissue was collected from three zones, the infarct zone, a peripheral zone of the injury, and a remote zone of healthy tissue. Sham operated animals were used as controls. Data normalized to *Gapdh*.

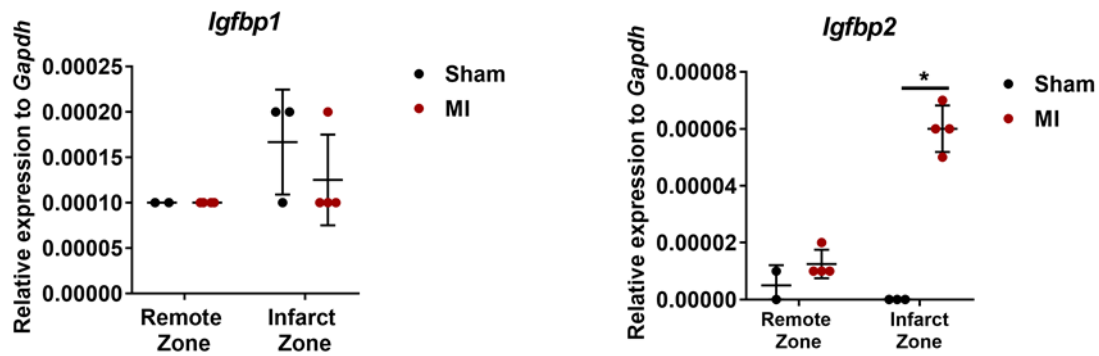


Figure S3 – IGF family is differently expressed after in the adult expression. Expression of *Igfbp1* and, *Igfbp2*, in sham and MI animals 96h after MI. Data was normalized to *Gapdh*, statistical significance was tested by One-way ANOVA, and *p* values for individual comparisons were calculated using the Tukey's test (sham n=4, MI n=5). Values are mean \pm SD * $p < 0.05$.

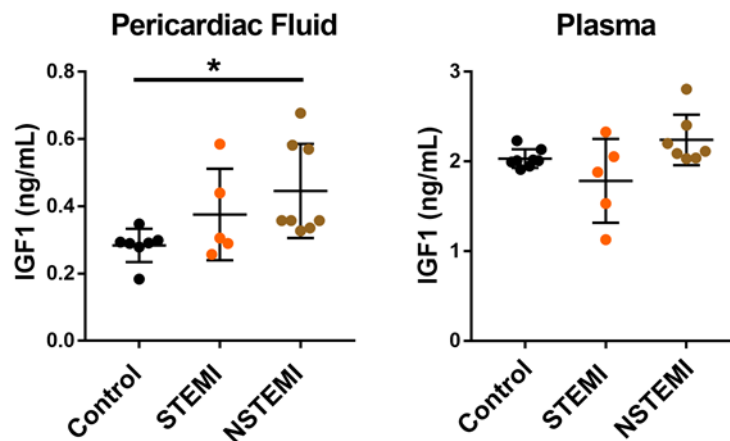


Figure S4 – IGF1 concentration in pericardiac fluid and plasma samples collected from MI and control patients quantified by an ELISA assay. Comparison between control patients, patients with MI STEMI (ST-elevation myocardial infarction), and patients with MI NSTEMI (non-ST-elevation myocardial infarction). Statistical significance was tested by non-parametric One-way ANOVA Kruskal-Wallis analysis, and *p* values for individual comparisons were calculated with Dunn's test. In the pericardiac fluid, a statistically significant difference was found between the NSTEMI and the control group (* $p = 0.0117$). This difference was not observed for the STEMI patients. No difference was found in plasma samples. Control n=8; STEMI n=5; NSTEMI n=7